RALF peptides modulate immune response in the moss *Physcomitrium patens*

Anna Mamaeva[1ǂ], Irina Lyapina[1ǂ], Andrey Knyazev[1], Nina Golub[1], Timur Mollaev[2], Elena Chudinova[2], Sergey Elansky[2,5], Vladislav V. Babenko[3], Vladimir A. Veselovsky[3], Ksenia M. Klimina[3], Tatiana Gribova[3], Daria Kharlampieva[3], Vassili Lazarev[3,4], Igor Fesenko[1*]

[ǂ]These authors contributed equally to this work and share first authorship

[1]Shemyakin and Ovchinnikov Institute of Bioorganic Chemistry, Russian Academy of Sciences, Moscow, Russia

[2]Peoples Friendship University of Russia (RUDN University), 117198, Moscow, Russia

[3]Federal Research and Clinical Center of Physical-Chemical Medicine of Federal Medical Biological Agency, Moscow, Russia

[4]Moscow Institute of Physics and Technology (National Research University), Dolgoprudny, Moscow region, 141701, Russia

[5]Lomonosov Moscow State University, 119991 Moscow, Russia

***Correspondence:**
Igor Fesenko
fesigor@gmail.com

Keywords: RALF, peptide, stress response, immunity

Abstract

RAPID ALKALINIZATION FACTOR (RALFs) are cysteine-rich peptides that regulate multiple physiological processes in plants. This peptide family has considerably expanded during land plant evolution, but the role of ancient RALFs in modulating stress response is unknown. Here, we used the moss *Physcomitrium patens* as a model to gain insight into the role of RALF peptides in coordination of plant growth and stress response in non-vascular plants. The quantitative proteomic analysis revealed concerted downregulation of M6 metalloproteases and some membrane proteins, including those involved in stress response, in *PpRALF1*, *2* and *3* knockout (KO) lines. We found that knockout of *PpRALF2* and *PpRALF3* genes resulted in increased resistance to bacterial and fungal phytopathogens - *Pectobacterium carotovorum* and *Fusarium solani*, suggesting the role of these peptides in negative regulation of immune response in *P. patens*. The comparative transcriptome analysis of *PpRALF3* KO and wild type plants under *Fusarium solani* infection showed the clear difference in regulation of genes belonging to phenylpropanoid pathway and associated with cell wall modification and biogenesis between these genotypes. The follow-up analysis revealed the role of PpRALF3 in growth regulation under abiotic and biotic stress regulation, which suggests the role of RALFs in responses to different adverse conditions. Thus, our study sheds light on the function of the previously uncharacterized PpRALF3 peptide and gives a clue to ancestral functions of RALF peptides in plant stress response.

1 Introduction

Plants utilize small secreted peptides as important mediators of many processes, from growth and development to response to stress conditions (Olsson et al., 2019). One of such regulators is the conservative 5 kDa peptide family - RALF (Rapid Alkalinization Factor), which are widely present in terrestrial plants (Campbell and Turner, 2017). The mature RALF peptide contains four cysteine amino acid residues which form two S-S bonds (Frederick et al., 2019). RALF peptides are cleaved from an inactive protein precursor and S1P protease is shown to be involved in the cleavage of a mature RALF peptide from a nonfunctional precursor at the conserved dibasic RR site (Srivastava et al., 2009; Stegmann et al., 2017).

The tandem duplication is considered to play a dominant role in the evolution of RALFs and this peptide family has expanded considerably during land plant evolution (Cao and Shi, 2012; Campbell and Turner, 2017). For example, 37 members of this family were found in *Arabidopsis thaliana*, 25 in *Arabidopsis halleri*, 20 in *Zea mays*, but only 3 in *Physcomitrium patens* (Campbell and Turner, 2017; Ginanjar et al., 2022). RALF peptides are diverged into four clades based on mature peptide region sequence features (Campbell and Turner, 2017). RALF peptides from I, II and III clades contain a specific protease cleavage site and conserved YISY motif, which is important for their recognition through receptors (Campbell and Turner, 2017; Xiao et al., 2019). However, RALF peptides from clade IV lack specific cleavage site, in addition, the conserved motif also changes, thus suggesting diverse functions of the representatives from this clade.

Unlike most other plant peptide hormones, RALF peptides bind to membrane-localized receptor-like kinases with malectin-like extracellular domain instead of leucine-rich repeat domain (Franck et al., 2018). Receptors of RALF peptides belong to the *Catharanthus roseus* receptor-like kinase (CrRLK1L) family and include FERONIA (FER), CrRLK1Ls ANXUR1 (ANX1), ANX2, and BUDDHA'S PAPER SEAL (BUPS) 1 and BUPS2 (Ge et al., 2017, 2019). In addition, LRE LIKE GPI-AP1 (LLG1) was proposed to function as a coreceptor for FER in AtRALF1 perception in Arabidopsis (Li et al., 2015). In bryophytes, such as *Marchantia polymorpha* L., *P. patens*, and *Sphagnum fallax* were identified 1, 5 and 7 CrRLK1Ls, respectively (Solis-Miranda et al., 2020). Also, LEUCINE-RICH REPEAT EXTENSINS (LRX) proteins are shown to bind RALF peptides with high affinity (Mecchia et al., 2017; Zhao et al., 2018; Moussu et al., 2020).

The diversity of receptors and co-receptors that can bind different RALF peptides results in their multiple functions and different signaling pathways activation (Abarca et al., 2021). RALF peptides are involved in the regulation of root growth, pollen tube elongation, formation of nitrogen-fixing nodules and inulin accumulation (Murphy and De Smet, 2014; Tena, 2016; Wieghaus et al., 2019). Also, they are involved in the processes of intercellular communication between sporophyte and gametophyte in land plants (Chevalier et al., 2013; Mecchia et al., 2017; Loubert-Hudon et al., 2020). The function of *RALF* genes that have been identified in bryophyte genomes are still being studied. PpRALF1 and PpRALF2 - out of three PpRALF peptides identified in *P. patens* have been shown to promote protonema tip growth and elongation (Ginanjar et al., 2022). Although, the function of PpRALF3 peptide is still unknown.

Besides regulation of growth and development, RALF peptides are also involved in the regulation of responses to abiotic and biotic stresses (Blackburn et al., 2020). For example, AtRALF8 plays a role in simultaneously controlling responses to drought and nematode attack by allegedly regulating cell wall remodeling (Atkinson et al., 2013). However, as has

been shown in Arabidopsis, different RALF peptides may have opposite effects. For example, AtRALF17 increases reactive oxygen species (ROS) production and resistance to *Pseudomonas syringae* pv. tomato, while AtRALF23 has the opposite effect (Stegmann et al., 2017). AtRALF33, a close relative of AtRALF23, was shown to inhibit pathogen elicitor-induced ROS production (Stegmann et al., 2017). In addition, AtRALF23 along with AtRALF22 were also shown to participate in regulation of growth and salt stress tolerance by cell wall remodeling (Zhao et al., 2018). The exogenous treatment with synthetic AtRALF1, AtRALF4, AtRALF19 and AtRALF22 reduces elicitor-induced ROS production (Abarca et al., 2021). The corresponding precursors of these AtRALFs contain an S1P cleavage site, but AtRALF6-13, AtRALF15-17, AtRALF20, AtRALF24, AtRALF29-32, AtRALF35-36, which reported to increase elf18-induced ROS production, are not cleaved by this protease (Abarca et al., 2021). Perhaps, the presence of S1P cleavage sites is linked to the negative regulation of the immunity with some exceptions (Stegmann et al., 2017; Abarca et al., 2021).

The participation of RALF peptides in modulation of the response to biotic stress has been shown not only in Arabidopsis, but also in other plants, including crops (Stegmann et al., 2017; Merino et al., 2019). Generally, RALF peptides are considered to be negative regulators of the immune response, which can be used by pathogens to promote infection. Considering that many pathogens, especially fungi, prefer alkaline conditions, the ability of RALFs to alkalize the environment came in very handy. Many plant pathogens synthesize RALF-like peptides that enhance the development of infection (Tena, 2016; Thynne et al., 2017). In tomato and *Nicotiana benthamiana* a synthetic RALF-like peptide from *Fusarium oxysporum* f. sp. *lycopersici* was able to induce ROS burst, alkalinization and activation of MAPKs as well as inhibit the seedlings growth (Thynne et al., 2017). Moreover, RALF-like peptides from plant root-knot nematodes facilitate the process of infection in Arabidopsis and rice (Zhang et al., 2020a). Although these homologs may have an arguable impact on the potency of pathogen infection (Wood et al., 2020).

The role of ancient RALF peptides in response to stress conditions is unknown. Meanwhile, the analysis of different plant lineages allows us to gain insight into their possible functions in regulation of stress response during terrestrialization. Using quantitative proteomic and transcriptomic analysis along with infection with *Pectobacterium carotovorum* and *Fusarium solani*, we studied the role of three PpRALF peptides from the model bryophyte *Physcomitrium patens* in immune stress response. Our study showed the specific role of PpRALF3 in negative regulation of plant stress response.

2 Materials and Methods

2.1 Plant growth conditions and treatments

Physcomitrella patens subsp. *patens* (*Physcomitrium patens* "Gransden 2004", Freiburg) protonemata were grown on BCD medium supplemented with 5 mM ammonium tartrate (BCDAT) and/or 0.5% glucose with 1.5% agar (Helicon, Moscow, Russian Federation) in a Sanyo Plant Growth Incubator MLR-352H (Panasonic, Osaka, Japan) with a photon flux of 61 μmol/m^2•s during a 16-hour photoperiod at 24°C in 9-cm Petri dishes (Nishiyama et al. 2000). For proteomic and qRT-PCR analyses, the protonemata were grown in liquid BCDAT medium and collected on day 7. The gametophores were grown on free-ammonium tartrate BCD medium under the same conditions, and 8-week-old gametophores were used for analysis. For resistance to abiotic stresses analyses, protonema was grown on BCD medium without ammonium tartrate supplemented with 150 mM NaCl or 2 mM PQ. For Pp*RALF*

genes expression analysis 7-days-old protonema was treated with 100 mM hydrogen peroxide for 2 hours.

For morphological analysis, protonema tissue 2 mm in diameter was planted on 9 cm Petri dishes on BCD and BCDAT media.

For growth rate measurements, photographs were taken at day 30 of subcultivation. Protonemal tissues and cells were photographed using a Microscope Digital Eyepiece DCM-510 attached to a Stemi 305 stereomicroscope.

2.2 Generation of knockout mutant lines

PpRALF1 (Pp3c3_15280V3), *PpRALF2* (Pp3c6_7200V3) and *PpRALF3* (Pp3c25_4180V3) knockout lines were created using the CRISPR/Cas9 system (Collonnier et al., 2017). The coding sequences were used to search for guide sequences preceded by a *S. pyogenes* Cas9 PAM motif (NGG) using the web tool CRISPOR (http://crispor.tefor.net/). The guide sequence closest to the translation start site (ATG) was selected for cloning (Supplementary Table S1 and Figure S1). These sequences were cloned into plasmid pBB (Fesenko et al., 2019), yielding the final complete sgRNA expression cassette. Protoplasts were obtained from protonemata as described previously (Fesenko et al., 2015) and transformed by PEG transformation protocol (Schaefer and Zrÿd, 1997) using mixture of three plasmids 1) one of the pBB plasmid carrying guide RNA expression cassette; 2) pACT-CAS9 carrying CAS9 gene; 3) pBNRF plasmid carrying resistance gene to G418. The plasmids pACT-CAS9 and pBNRF were kindly provided by Dr. Fabien Nogué. Independent knockout mutant lines have been obtained. Double knockout lines were obtained by simultaneous transformation with two plasmids with the corresponding guide RNAs.

2.3 DNA and RNA isolation and quantitative reverse transcription PCR (qRT-PCR)

Genomic DNA from gametophores was isolated using a commercial kit (Biolabmix, Russia), according to the manufacturer's recommendations. Total RNA from gametophores and protonemata was isolated using TRIzol™ Reagent according to the manufacturer's recommendations. RNA quality and quantity were evaluated using electrophoresis on agarose gel with SYBR Green (Biolabmix, Russia). Total RNA concentration of samples was precisely measured using a Nanodrop™One (Thermo Fisher Scientific, USA).

cDNA was synthesized using the MMLV RT kit (Evrogen, Russian) according to the manufacturer's recommendations. OligodT primers were used to prepare cDNA from 2 µg total RNA after DNase treatment.

Real-time PCR was performed using the HS-qPCR SYBR Blue (2x) (Biolabmix, Russia) on a LightCycler®96 (Roche, Germany). qPCR was carried out in three biological and three technical replicates. Primers for *PpRALF* genes could be found in Supplementary Table S1.

For qPCR analysis of infection severity, primers were designed for *F. solani* or selected from previous research (Kabir et al., 2020) for *P. carotovorum* to specifically amplify pathogenic DNA from the infected moss plants (Supplementary Table S1).

169 **2.4 Pathogen inoculation and treatments**

170 Phytopathogens *Pectobacterium carotovorum subsp. atrosepticum* and *Fusarium solani* were
171 used to infect moss plants. Sterile water-treated plants were used as a control. For bacterial
172 treatment by spraying 15 µl of pre-prepared overnight culture with final concentration
173 9.5×10^6 cfu/ml were used. *F. solani* spores were obtained from a solid medium culture and
174 applied by spraying the suspension with final concentration 8.3×10^5 spores/ml. Petri dishes
175 with infected plants were cultivated at room temperature under standard daylight conditions
176 (16h day/8h night). Infected plants were collected after 7 days and frozen in liquid nitrogen.

177 **2.5 Protein extraction and trypsin digestion**

178 Protein extraction and trypsin digestion we conducted as described previously (Faurobert et
179 al., 2007; Fesenko et al., 2021b). iTRAQ labeling (Applied Biosystems, Foster City, CA,
180 USA) was conducted according to the manufacturer's manual. Proteins were labeled with the
181 iTRAQ tags as follows: Wild type biological replicates – 113, 114, 115 isobaric tags;
182 *PpRALF1*, *PpRALF2* and *PpRALF3* KO biological replicates – 116, 117, 118 isobaric tags
183 for each mutant line.

184 **2.6 LC-MC/MC analysis and protein identification and quantification**

185 The LC–MS/MS analysis was performed as described earlier (Fesenko et al., 2021a). Tandem
186 mass spectra were searched with PEAKS Studio version 8.0 software (Bioinfor Inc., CA,
187 USA) against a custom database containing 32 926 proteins from annotated genes in the latest
188 version of the moss genome v3.3 (Lang et al., 2018), 85 chloroplast proteins and 42
189 mitochondrial proteins. The search parameters were the following: a fragmentation mass
190 tolerance of 0.05 Da; parent ion tolerance of 10 ppm; fixed modification –
191 carbamidomethylation; variable modifications - oxidation (M), deamidation (NQ), and
192 acetylation (Protein N-term). The results were filtered by a 1% FDR, but with a significance
193 threshold not less than 20 (equivalent is P-value < 0.01). The results were filtered by a 1%
194 false discovery rate (FDR). PEAKS Q was used for iTRAQ quantification. Normalization
195 was performed by averaging the abundance of all peptides. Median values were used for
196 averaging. Although iTRAQ quantification usually underestimates the amount of real fold
197 changes between two samples (Ow et al., 2009), we used a very strict filter for differentially
198 expressed proteins. The threshold for calling a protein differentially abundant was calculated
199 based on an s0 parameter (s0=0.1) as described previously (Schessner et al., 2022) with a
200 permutation test repeated 100 times and Benjamini and Hochberg FDR correction (FDR_BH
201 < 1%).

202 **2.7 RNA-seq analysis**

203 DNase treatment was carried out with TURBO DNA-free kit (Thermo Fisher Scientific,
204 Waltham, MA, USA), in volumes of 50 µl. RNA cleanup was performed with the Agencourt
205 RNA Clean XP kit (Beckman Coulter, Brea, USA). The concentration and quality of the total
206 RNA were checked by the Quant-it RiboGreen RNA assay (Thermo Fisher Scientific) and
207 the RNA 6000 Pico chip (Agilent Technologies, Santa Clara, CA, USA), respectively.

208 RNA libraries were prepared using NEBNext Poly(A) mRNA Magnetic Isolation Module
209 and the NEBNext Ultra II Directional RNA Library Prep Kit (NEB), according to the
210 manufacturer's protocol. The library underwent a final cleanup using the Agencourt AMPure
211 XP system (Beckman Coulter) after which the libraries' size distribution and quality were
212 assessed using a high sensitivity DNA chip (Agilent Technologies). Libraries were

213 subsequently quantified by Quant-iT DNA Assay Kit, High Sensitivity (Thermo Fisher
214 Scientific). Finally, equimolar quantities of all libraries (10 pM) were sequenced by a high
215 throughput run on the Illumina HiSeq 2500 using 2 × 100 bp paired-end reads and a 1% Phix
216 spike-in control.

217 The adaptors and low-quality sequences were removed from raw reads by Trimmomatic
218 v0.39 (Bolger et al., 2014). Clean reads were aligned to the *P. patens* v3.3 reference genome
219 (download from the website: https://phytozome-next.jgi.doe.gov) using HISAT2 v2.1.0 (Kim
220 et al., 2015) and the alignments were sorted with Samtools (Li et al., 2009). The expression
221 abundances of mapped reads were counted by the FeatureCounts tool (Liao et al., 2014).
222 Differential expression analysis was performed by EdgeR package (Robinson et al., 2010).
223 The genes were defined as differentially expressed genes (DEGs) with adjusted p-value ≤
224 0.05 and fold change ≥1.0.

225 **2.8 Cell wall staining and fluorescence microscopy**

226 Protoplasts were prepared from protonemata as described previously (Fesenko et al. 2015)
227 and incubated for 48 h at solid BCD agar medium. Regenerated protoplasts were dyed with
228 10 mkg/ml Calcofluor White (Fluorescent Brightener 28) for 5 min. The fluorescence was
229 analyzed using fluorescent microscope (Axio Imager M2, Zeiss, Germany) at λex = 365 nm,
230 BS FT 395, and λem = 445nm /50 nm (Filter set 49 DAPI, Zeiss, Germany).

231 To detect intracellular ROS, we used the fluorescent dye 2′,7′-Dichlorofluorescin Diacetate
232 (DCFH-DA, Sigma-Aldrich, USA). Seven-days old protonema filaments were harvested with
233 a spatula from the agar surface and placed into mQ. Protonema was then treated with
234 0.0025% driselase 1 min and incubated with 10 µM DCFH-DA for 15 min in total. The No.
235 44 filter (λex BP 475 nm/40 nm; λem BP 530 nm/50 nm) was used for DCFH-DA
236 fluorescence detection on the fluorescent microscope Axio Imager M2 (Zeiss) with an
237 AxioCam 506 mono digital camera. Data on the fluorescence intensity were obtained from
238 the related Zeiss software Zen.

239 **2.9 Bioinformatic analysis**

240 Protein–protein interaction networks were constructed using STRING v.10 (www.string-
241 db.org) with the default options (Szklarczyk et al., 2014). The visualization of the protein
242 interaction was performed with Cytoscape software (Shannon et al., 2003). The GO
243 enrichment analysis was conducted by g:Profiler (Raudvere et al., 2019). Multiple alignments
244 were created using the MAFFT algorithm (Katoh et al., 2019) and visualized using Jalview
245 software (Waterhouse et al., 2009). Principal Component Analysis (PCA) was performed
246 using iFeature tool (Chen et al., 2018).

247 **2.10 Statistics**

248 Statistical analysis and visualization were made in Python v. 3.7.5 (Van Rossum and Drake,
249 1995) using modules scipy 1.5.2 (Virtanen et al., 2020), seaborn 0.11.1 (Waskom, 2021),
250 numpy 1.20.1, pandas 1.2.3 (McKinney, 2012). For two- or more-way analysis of variance
251 (ANOVA), Tukey's honestly significant difference (HSD) tests based on multiple
252 comparisons of means were applied to determine which pairwise comparisons were
253 statistically significant. Differences were considered to be significant at $p < 0.05$.

3 Results

3.1 The amino acid composition of PpRALFs

The members of a RALF peptide family possess functional heterogeneity in vascular plants (Blackburn et al., 2020), including the role in modulation of immune response. In Arabidopsis, exogenous application of synthetic AtRALF23, AtRALF33, AtRALF34 are shown to inhibit production of reactive oxygen species (ROS) induced upon treatment with immune elicitors (such as elf18) and inhibit seedling and root growth, whereas AtRALF17, AtRALF24, AtRALF32 and some others were able to induce ROS production (Abarca et al., 2021). The previous phylogenetic analysis divided the RALFs into four clades and peptide sequences from different clades could be distinguished based on analysis of their physico-chemical properties (Campbell and Turner, 2017). To test how overall amino acid composition of RALF peptides is related to their possible functions, we used Principal Component Analysis (PCA) to cluster PpRALFs and AtRALFs together. This analysis revealed a clear pattern, in which AtRALF peptides with different effects on pathogen-induced ROS production were separated from each other (Figure 1A). PpRALFs were clustered with AtRALFs that inhibit elicitor-induced ROS production (Abarca et al., 2021). These results are consistent with data of previous phylogenetic analysis (Ginanjar et al., 2022), where PpRALFs were grouped with AtRALF23, AtRALF33, AtRALF23, AtRALF22. These findings suggest that overall amino acid composition of RALF peptides, to some extent, reflect their functional biases and PpRALFs are related to AtRALFs that negatively regulate immune response.

In *Physcomitrium patens*, PpRALF1 and PpRALF2, that belong to Clade III (Campbell and Turner, 2017), have shown to promote protonema tip growth and elongation (Ginanjar et al., 2022). However, the third member of RALF peptide family - PpRALF3 was not analyzed in Campbell and Turner 2017 and has substitution in conserved "RGC" motif (Figure 1B). The AtRALFs that were clustered together with PpRALF peptides (Figure 1A) belong to Clades 1, 2 and 3 (Campbell and Turner, 2017), implying the absence of the correlation between RALF functions in immune response and division into clades in this case. However, the role of PpRALFs in response to stress conditions is unknown.

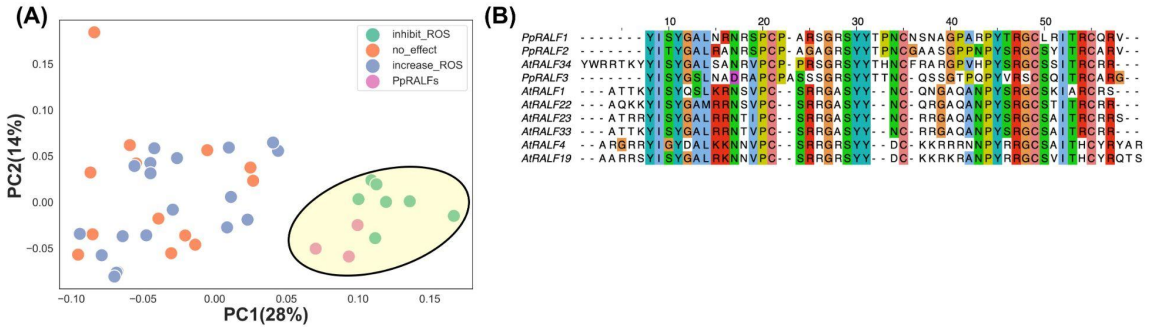

Figure 1. **(A)** - Principal Component Analysis (PCA) of amino acid composition, calculated by iFeature tool (Chen et al., 2018) for AtRALF and PpRALF peptides. Moss PpRALFs were clustered with reported immune-related RALF peptides from Arabidopsis, such as AtRALF1, AtRALF4, AtRALF19, AtRALF22, AtRALF23, AtRALF33, AtRALF34. **(B)** - The multiple

288 pairwise alignment of PpRALFs and immune-related AtRALFs (AtRALF19, AtRALF34,
289 AtRALF33, AtRALF23, AtRALF22).

290 **3.2 The knockout of *PpRALF*s resulted in changes of cell wall-associated proteins**

291 PpRALF1 and PpRALF2 peptides are previously shown to promote tip growth and
292 elongation of protonemata filaments in *P. patens*, but the functions of PpRALF3 peptide are
293 currently unknown (Ginanjar et al., 2022). The chemical synthesis of RALF peptides, as well
294 as the generation of recombinant peptides, is associated with certain difficulties. Proper
295 bonding and folding of peptides require the right conditions, otherwise peptides may not
296 work the way they do, or a higher concentration could be required (Abarca et al., 2021).
297 Since this may not reflect the actual effect of the peptides, we decided to use only knockout
298 lines. At least two independent knockout lines for each *PpRALF* gene and double knockout
299 lines - *PpRALF1* and *PpRALF3*; *PpRALF2* and *PpRALF3* were generated by CRISPR/Cas9
300 technology (Table 1). However, we failed to obtain triple and double *PpRALF1* and
301 *PpRALF2* knockout lines after several attempts. Probably, this is due to their important roles
302 in regulation of moss growth and development.

303

304 **Table 1. The list of obtained mutant lines**

Phytozome ID	**Name**	**The number of mutant lines**
Pp3c3_15280	*PpRALF1 KO*	2
Pp3c6_7200	*PpRALF2 KO*	2
Pp3c25_4180	*PpRALF3 KO*	2
Pp3c3_15280, Pp3c25_4180	*PpRALF1,3 KO*	1
Pp3c6_7200, Pp3c25_4180	*PpRALF2,3 KO*	1

305

306 It has been previously shown that knockout of *PpRALF* genes results in reducing the
307 formation of caulonema filaments (Ginanjar et al., 2022). Therefore, we tested the growth of
308 our mutants on medium with and without ammonium tartrate (BCDAT/BCD; Figure 2A).
309 The ammonium tartrate reduces the transition into caulonemal cells and promotes
310 chloronemal branching (Vidali and Bezanilla, 2012). The morphology of wild type and single
311 knockout mutants was similar, but the diameter of *PpRALF3* KO plants was significantly
312 larger than wild types on the BCDAT medium (Figure 2A and 2B; ANOVA with post-hoc
313 Tukey HSD $P < 0.001$). In contrast, the growth rate of *PpRALF1* KO lines did not differ from
314 wild type on all media examined (Figure 2A and 2B). In addition, *PpRALF2* KO plants were
315 significantly smaller than wild type plants on the medium with ammonium tartrate (Figure
316 2B, ANOVA with post-hoc Tukey HSD $P < 0.001$). Both double knockouts showed
317 significant inhibition of the growth rate on medium with and without ammonium tartrate

318 (Figure 2A and 2B; ANOVA with post-hoc Tukey HSD $P < 0.001$). In addition, the
319 gametophores were significantly longer in both *PpRALF3* KO lines in comparison to other
320 genotypes (Supplementary Figure S2; ANOVA with post-hoc Tukey HSD $P < 0.001$). Thus,
321 our results are in line with previously obtained data on morphology and phenotypes of
322 *PpRALF* knockouts (Ginanjar et al., 2022). In addition, our results suggest that all PpRALFs
323 are functional and might play different roles, beyond the regulation of only growth processes.

324 Using isobaric tags for relative and absolute quantification (iTRAQ), we further compared
325 proteomes of *PpRALF1*, *PpRALF2*, *PpRALF3* knockout lines and wild type plants. In total,
326 we identified 2723 protein groups in *PpRALF1* KO, 3074 protein groups in *PpRALF2* KO
327 and 3078 protein groups in *PpRALF3* KO (Supplementary Table S2). Although iTRAQ
328 quantification usually underestimates the amount of real fold changes between two samples
329 (Ow et al., 2009), we used a very strict cut-off to reliably identify differentially expressed
330 protein groups (DEPs), such as an s0 parameter equal 0.1 and multiple hypothesis correction
331 that was performed based on a permutation test (see Methods). In contrast to previously
332 published transcriptomes of the *PpRALFs* knockout lines (Ginanjar et al., 2022), we have not
333 identified substantial changes in knockout proteomes in comparison to wild type plants,
334 suggesting primarily regulatory roles of PpRALF peptides. In *PpRALF1* KO plants only 8
335 protein groups were significantly changed (FDR BH < 1%, s0=0.1; Figure 2C;
336 Supplementary Table S2) in comparison to wild type plants and all of these DEPs were
337 downregulated. The knockout of PpRALF2 peptide resulted in downregulation of 15 protein
338 groups (FDR_BH < 1%, s0=0.1; Figure 2C; Supplementary Table S2) and upregulation of an
339 uncharacterized 257 aa protein Pp3c16_14730, containing predicted signal peptide. In
340 *PpRALF3* KO plants only 5 protein groups were significantly downregulated (FDR_BH <
341 1%, s0=0.1; Figure 2C; Supplementary Table S2).

342 We further compared these DEPs from all knockout lines and found a core set of four
343 proteins that were changed in at least two single-gene knockout lines. For example, we
344 revealed that a protein Pp3c15_830 (M6 family metalloprotease domain-containing protein)
345 was downregulated in *PpRALF1*, *PpRALF2* and *PpRALF3* KO lines. However, the role of
346 such proteins in RALF signaling has not been previously described. Another DE protein that
347 belonged to M6 metalloproteases - Pp3c13_22390 was downregulated only in the *PpRALF1*
348 KO line. We also identified two proteins that were downregulated in both *PpRALF1* and
349 *PpRALF2* KO lines. One of them - Pp3c26_120 (Bryoporin) is known to be important for a
350 response to osmotic stress in mosses (Hoang et al., 2009). The other uncharacterized protein -
351 Pp3c14_22870 has orthologs that were characterized as Hydrophobic surface binding
352 proteins (HsbA) in other moss species. We also identified LOX3 protein (Pp3c15_13040)
353 that downregulated in *PpRALF2* and *PpRALF3* KO lines, which might be involved in the
354 arachidonic acid metabolism, suggesting the possible role of these paralogs in biotic stress
355 response.

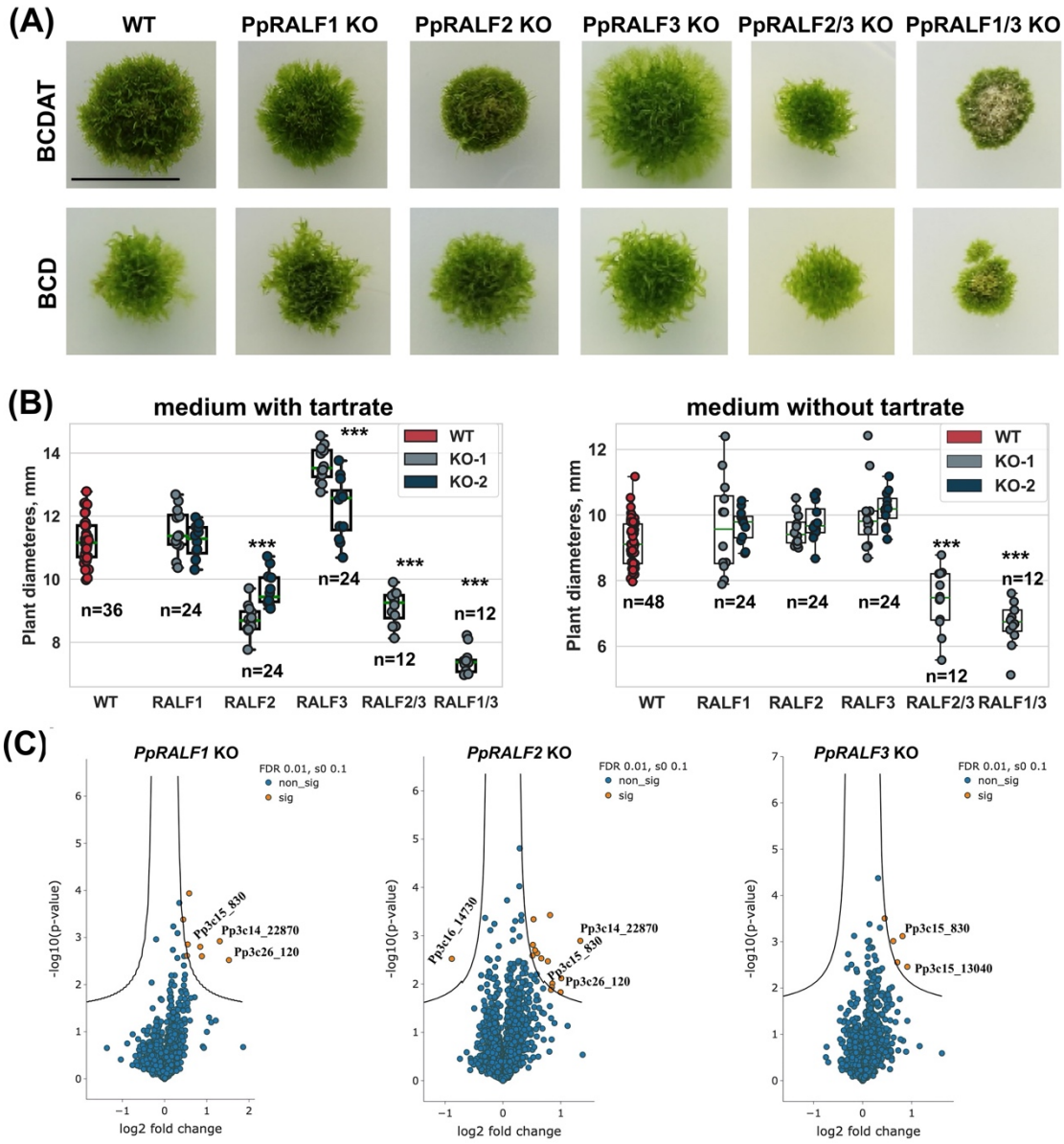

Figure 2. (A) - Phenotype of 30-d-old plants of wild type and the obtained knockout lines grown on two mediums with and without ammonium tartrate; **(B)** - The measured diameter of wild type and knockout lines grown on mediums with (left) and without ammonium tartrate (right). Analysis of variance and Tukey's HSD post hoc tests were performed ***$P < 0.001$; **(C)** - Volcano plots of the entire set of proteins quantified during iTRAQ analysis of *PpRALF1*, *PpRALF2* and *PpRALF3* KO lines, respectively. Proteins significantly changed in abundance are depicted in orange; Pp3c15_830 - M6 family metalloprotease domain-containing protein, Pp3c14_22870 - Hydrophobic surface binding protein (HsbA), Pp3c26_120 - bryoporin, Pp3c15_13040 - 12-lipoxygenase, Pp3c16_14730 - Stigma-specific protein, Stig1.

Thus, the knockout of *PpRALF* genes resulted in downregulation of some proteases and previously uncharacterized membrane proteins. To determine whether these changes in proteomes of mutant lines affected the cell wall regeneration processes, we explored the process of protoplast regeneration in the knockout and wild type genotypes. The protoplasts

371 were dyed with Calcofluor White fluorescent dye that is widely used to visualize cellulose,
372 callose, and other β-glucans in the plant cell wall (Maksimov et al., 2016; Herrera-Ubaldo
373 and de Folter, 2018). On average, the cell wall regenerated 80% faster in *PpRALF2* KO lines
374 (chi-square $P < 0.001$) and 46% faster in *PpRALF3* KO lines (chi-square $P < 0.001$) than in
375 wild type cells after two days of regeneration process (Supplementary Figure S3). We found
376 no significant differences in the cell wall regeneration rate between *PpRALF1* KO-1 and wild
377 type plants.

378 **3.3 The *PpRALF3* knockout lines are more tolerant to abiotic stress factors**

379 Some members of the RALF peptide family are shown to modulate the abiotic stress response
380 in angiosperms (Zhao et al., 2018). Therefore, we next sought to expand our understanding of
381 PpRALFs functions under abiotic stress conditions. At first, we used previously obtained
382 RNA-seq data (Khraiwesh et al., 2015) to analyze the expression of *PpRALF* genes under
383 salt, drought, and cold treatments. According to this study, *PpRALF1* was significantly
384 upregulated in all stress conditions after 0.5 h and under cold treatment after 4h but
385 downregulated under drought and salt treatment after 4 h. In addition, the *PpRALF2* gene was
386 significantly upregulated at drought after 0.5 h and at cold after 4 h as well. The *PpRALF3*
387 transcripts were detected only under salt and drought treatment, suggesting its possible role in
388 stress response.

389 We also assessed the transcriptional level of all *PpRALFs* under hydrogen peroxide treatment
390 for 2 hours. According to qRT-PCR, all *PpRALFs* were significantly downregulated under
391 this treatment (Figure 3A; ANOVA with post-hoc Tukey HSD $P < 0.001$). However, the
392 transcriptional level of *PpRALF3* decreased less than that of other *PpRALFs.*

393 Taking into account the role of RALF peptides, such as AtRALF22/23, in regulation of salt
394 stress tolerance in Arabidopsis (Zhao et al., 2018), we further assessed the growth rate of
395 *PpRALF* KO plants upon the oxidative (2 mM paraquat) and salt (150 mM NaCl) treatments.
396 We have chosen the salt concentration of 150 mM NaCl for these experiments based on our
397 assessment of wild type plant phenotypes upon different salt concentrations (Supplementary
398 Figure S4). Our experiments showed that wild type and knockout plants were affected by 150
399 mM NaCl, confirming the adverse effect of high salt concentration on moss growth and
400 development (Figure 3B). Herewith, the growth rate of wild type and *PpRALF1* and *2* KO
401 plants was similar under salt treatment, except for *PpRALF3* KO lines. The diameter of
402 *PpRALF3* KO lines was significantly larger (ANOVA with post-hoc Tukey HSD $P < 0.001$)
403 under salt treatments compared to mock treated and wild type plants due to diffusion of
404 protonemal filaments (Figure 3B and C). These findings suggest the role of PpRALF3 in the
405 response to abiotic stress factors, as has been shown for angiosperm RALFs. For example,
406 overexpression of AtRALF22 or AtRALF23 has previously been shown to increase
407 sensitivity to salt stress (Zhao et al., 2018).

408 Under the oxidative stress conditions, the growth and morphology of both wild type and
409 mutant plants were severely affected (Figure 3B). The growth rate of *PpRALF1* and
410 *PpRALF2* KO lines was also significantly suppressed in comparison to normal conditions
411 (Figure 3B and C; ANOVA with post-hoc Tukey HSD $P < 0.001$). However, only the growth
412 of *PpRALF3* KO-2 plants was significantly reduced in comparison to normal conditions
413 (Figure 3C; ANOVA with post-hoc Tukey HSD $P < 0.001$) and both *PpRALF3* mutant lines
414 grew better than wild type. In addition, both double KO mutant lines were less sensitive to
415 paraquat in comparison to wild type plants (Figure 3C). Thus, our results showed that

416 *PpRALF3* is responsive to adverse conditions and its knockout lines are more tolerant to
417 growth inhibition during abiotic stress response.

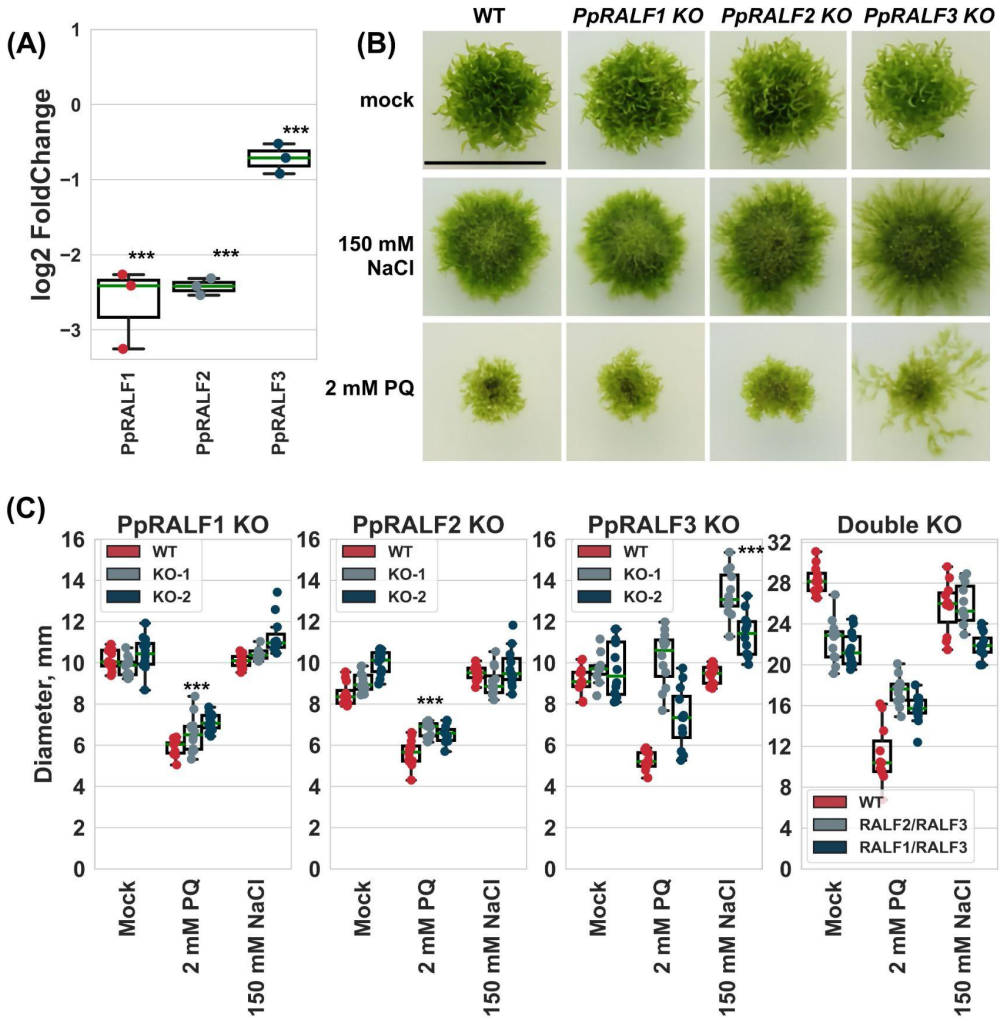

418

419 **Figure 3. (A)** - The results of quantitative reverse transcription PCR (RT-qPCR) analysis of
420 the transcriptional level of *PpRALFs* under hydrogen peroxide treatment for 2 hours.
421 Analysis of variance and Tukey's HSD post hoc tests were performed ***$P < 0.001$; **(B)** -
422 Phenotype of 30-d-old plants of wild type and the knockout lines grown on medium
423 supplemented with 150 mM NaCl or 2 mM paraquat; **(C)** - The measured diameter of moss
424 plants grown on medium supplemented with 150 mM NaCl or 2 mM paraquat. Analysis of
425 variance and Tukey's HSD post hoc tests were performed ***$P < 0.001$.

426 **3.4 The knockout of *PpRALF2* and *PpRALF3* increases resistance to**
427 **phytopathogens**

428 It has been previously shown that some RALF peptides can modulate immune response in
429 vascular plants (Stegmann et al., 2017; Zhang et al., 2020b; Abarca et al., 2021). For
430 example, treatment with AtRALF peptides increased or reduced ROS production under
431 induction of immune response by elf18 (Abarca et al., 2021). To determine whether the
432 knockout of *PpRALF* genes interfere with immune response in bryophytes, we next analyzed
433 ROS production in *P. patens* wild type and knockout lines under driselase treatment. We

434 found that ROS production was significantly reduced in *PpRALF1* and *PpRALF2* KOs in
435 comparison to wild type plants and *PpRALF3* knockout line after driselase treatment (Figure
436 4A; ANOVA with post-hoc Tukey HSD $P < 0.001$). Moreover, the background level of ROS
437 production in the *PpRALF3* knockout lines without treatment was significantly higher than in
438 the other genotypes (Figure 4A; ANOVA with post-hoc Tukey HSD $P < 0.001$). That may be
439 explained by the fact that PpRALF3 plays a role in suppressing the immune response. This is
440 in concordance with our PCA analysis where PpRALFs tend to cluster with AtRALFs that
441 decrease pathogen-induced ROS production (Figure 1A).

442 We further studied the possible functions of PpRALFs in defense response against
443 phytopathogens. For this, we infected moss plants with two well-known phytopathogens -
444 *Pectobacterium carotovorum subsp. atrosepticum* and *Fusarium solani*, which are mildly
445 aggressive and keep plants alive (Figure 4B). These pathogens also show distinct symptoms
446 of infection, such as brown spots caused by tissue necrosis (Akita et al., 2011; Alvarez et al.,
447 2016). To test whether the colonization and growth of *P. carotovorum* and *F. solani* differ
448 between wild type and knockout lines, moss plants were collected at 7 days post inoculation
449 (dpi) and the ratio of pathogen DNA to plant DNA concentrations was measured using
450 quantitative PCR analysis as was described previously (Castro et al., 2016).

451 According to our experiments, *P. carotovorum* growth rate was significantly higher in wild
452 type plants compared to *PpRALF2* KO and *PpRALF3* KO mutant lines (Figure 4C; ANOVA
453 with post-hoc Tukey HSD $P < 0.001$). However, the difference in *P. carotovorum* growth rate
454 between wild type and *PpRALF1* KO plants was not significant (Figure 4C). The growth of
455 *F. solani* was significantly reduced in all *PpRALF* knockouts in comparison to wild type
456 plants (Figure 4C; ANOVA with post-hoc Tukey HSD $P < 0.001$). Herewith, *PpRALF2* KO
457 and *PpRALF3* KO mutant lines were the most resistant to *F. solani* infection. Taken together,
458 these results indicated that knockout of *PpRALF* genes increased resistance of *P. patens* to
459 phytopathogens. Apparently, the PpRALF2 and PpRALF3 play a key role in negative
460 regulation of immune response in *P. patens* as was shown for some members of the RALF
461 family in Arabidopsis.

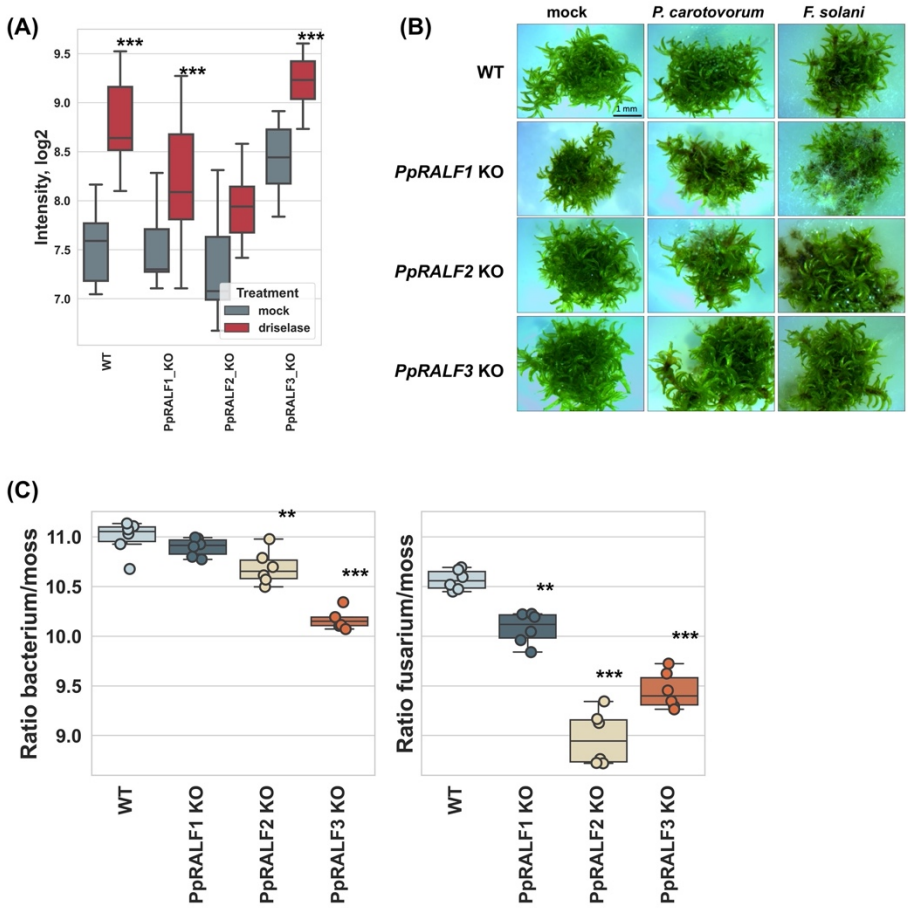

Figure 4. (**A**) **-** Effect of PpRALF peptide knockouts on ROS production in wild type and knockout lines under treatment with immune elicitors; **(B)** - Symptom development at 7 dpi in wild type, *PpRALF1*, *PpRALF2* and *PpRALF3* KO moss plants; **(C)** - Ratios of *P. carotovorum* and *F. solani* DNA levels to *P. patens* genomic DNA that were estimated by qPCR analysis. The results of six independent experiments are shown. Analysis of variance and Tukey's HSD post hoc tests were performed for qPCR data. $^{**}P < 0.01$, $^{***}P < 0.001$.

3.5 Transcriptome response during *F. solani* infection in *PpRALF3* KO line

According to our analysis, *PpRALF2* and *3* KO genotypes were more resistant to phytopathogens than wild type plants and *PpRALF1* knockout lines. To expand our understanding of the roles of PpRALFs in immune stress response, we next sought to perform RNA sequencing (RNA-seq) analysis to compare transcriptome response of *PpRALF3* KO and wild type plants during *F. solani* infection. Twelve paired-end RNA-Seq libraries were generated from three biological replicates of mock-inoculated and *F. solani*-infected wild type and *PpRALF3* KO plants (Supplementary Table S3). Overall, we detected more than 1700 differentially regulated genes (DEGs; $-1 \leq \log2$ fold change ≥ 1, $Padj < 0.05$) in both genotypes and 474 DEGs were commonly regulated in wild type and knockout plants (Figure 5A; Supplementary Table S4). These DEGs were changed in a similar manner in both wild type and knockout plants (Figure 5B). We further used the g:Profiler (Kolberg et al., 2020) for finding enriched GO terms in the set of commonly regulated DEGs (Figure 5C). These DEGs were mainly enriched in such GO terms as oxidoreductase activity (GO:0016491), response to reactive oxygen species (GO:0000302), antioxidant activity (GO:0016209;

484 Supplementary Table S5). These GO terms include genes involved in detoxification of
485 oxygen radicals, such as superoxide dismutase (Pp3c17_14510) or superoxide dismutase 1
486 copper chaperone (Pp3c17_14500) and producing lignin-like compounds, such as cinnamyl
487 alcohol dehydrogenases (Pp3c7_12220). These findings corroborate previous data obtained
488 during transcriptome analysis of the interaction between *Physcomitrium patens* and *Botrytis*
489 *cinerea* (Reboledo et al., 2021). We also identified some members of the EXPANSIN protein
490 family, such as Pp3c11_12000 (expansin 5-related) and Pp3c7_12870 (expansin 5-related)
491 that were upregulated in infected plants.

492 We next analyzed the differences in transcriptomic responses between examined genotypes.
493 In wild type plants, most of the top ten significantly enriched GO terms belonged to
494 secondary metabolite biosynthetic processes, including polyketide metabolic process
495 (GO:0030638), phenylpropanoid metabolic process (GO:0009698), cinnamic acid metabolic
496 process (GO:0009803; Figure 5D). The upregulated DEGs belonged to these GO terms
497 included histidine and phenylalanine ammonia-lyases (e.g. Pp3c13_9000) and chalcone
498 synthases (e.g. Pp3c11_9040, Figure 5F). In addition, the transcriptional level of genes
499 encoding heat shock proteins increased in wild type plants. The downregulated DEGs
500 identified in wild type plants were enriched in photosynthesis (GO:0015979). This is in line
501 with the previous study on the interaction between *P. patens* and *B. cinerea* (Reboledo et al.,
502 2021).

503 In contrast, the GO terms of downregulated genes in *PpRALF3* knockout line were
504 predominantly enriched in processes related to cell wall organization and biogenesis, such as
505 pectin catabolic process (GO:0045490), xyloglucan metabolic process (GO:0010411),
506 polysaccharide metabolic process (GO:0005976; Figure 5F). For example, groups of pectate
507 lyases (e.g. Pp3c21_16990) and pectin esterases were identified in this set of DEGs (Figure
508 G). The upregulated DEGs were enriched by such GO terms as oxidoreductase activity
509 (GO:0016491) and cell wall organization or biogenesis (GO:0071554). The latter included
510 pectin esterases, different glycosyl hydrolases and expansins.

511 In conclusion, transcriptomic changes in wild type plants are in line with previous data on *P.*
512 *patens* response to phytopathogens (Reboledo et al., 2021) and alter such processes as ROS
513 production and detoxification, biosynthesis of secondary metabolites with different roles in
514 defense and some others. The remarkable difference between *PpRALF3* KO and wild type
515 plants consisted of transcriptomic changes in genes related to cell wall modification and
516 biogenesis processes. Considering the known role of RALF peptides in cell wall remodeling,
517 it can be suggested that these changes during infection result from knockout of *PpRALF3*
518 gene.

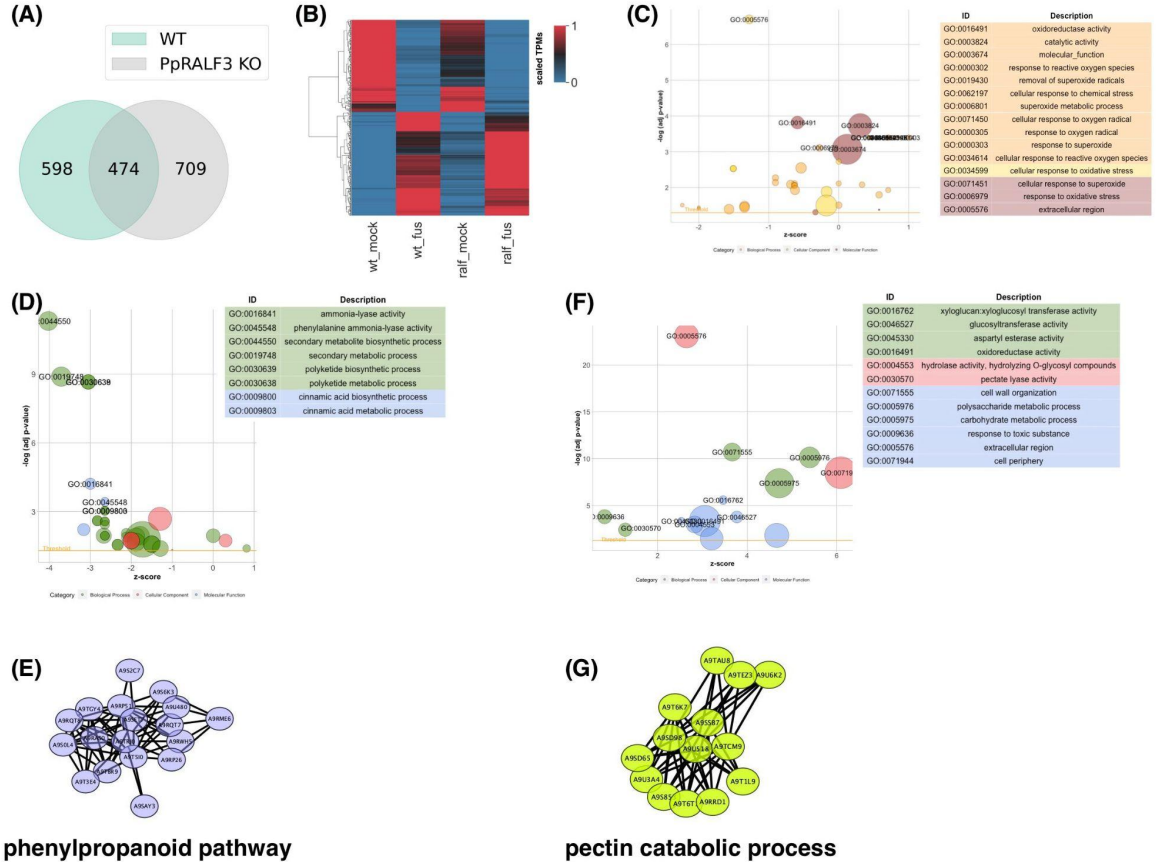

Figure 5. (**A) -** Venn diagram shows overlapping differentially regulated genes (DEGs; 1 ≤ log2 fold change ≥ 1, *Padj* < 0.05) between wild type and *PpRALF3* KO lines; **(B)** - Heatmap that depicts the euclidean-distance clustering analysis of overlapped DEGs. wt_mock - scaled mean TPM in wild type mock plants, wt_fus - scaled mean TPM in wild type infected plants, ralf_mock - scaled mean TPM in *PpRALF3* KO mock plants, ralf_fus - scaled mean TPM in *PpRALF3* KO infected plants; **(C)** - A bubble plot that depicts enriched GO terms (false discovery rate (FDR) adjusted *P*-values ≤ 0.05) for overlapped DEGs between wild type and *PpRALF3* KO lines; **(D)** - A bubble plot that depicts enriched GO terms in wild type plants. - Log adj p-values are shown in y-axis and z-scores are shown in x-axis. Size of the bubbles is proportional to the number of DEGs; **(E)** - Protein–protein interaction networks of a group of upregulated differentially expressed genes in wild type plants that belong to phenylpropanoid metabolic process. Genes are indicated with nodes, and interactions between proteins are represented by edges; **(F)** - A bubble plot that depicts enriched GO terms in *PpRALF3* KO plants. - Log adj p-values are shown in y-axis and z-scores are shown in x-axis. Size of the bubbles is proportional to the number of DEGs; **(G)** - Protein–protein interaction networks of a group of downregulated differentially expressed genes in *PpRALF3* KO plants that belong to pectin catabolic process. Genes are indicated with nodes, and interactions between proteins are represented by edges.

4 Discussion

RAPID ALKALINIZATION FACTOR (RALF) peptides are ubiquitous for land plants, including *Physcomitrium patens* and *Selaginélla moellendorffii*, but were not identified in chlorophyte species (Campbell and Turner, 2017). In angiosperms, RALFs are shown to modulate responses to biotic and abiotic stresses (Blackburn et al., 2020), but it is currently

543 unknown if ancient RALF peptides helped plants to cope with different stress factors or if the
544 immune-related RALFs appeared later as a result of tandem duplication and diversification
545 (Cao and Shi, 2012). Here, we investigated the role of three PpRALF peptides from the
546 model bryophyte *P. patens*, named as PpRALF1 (Pp3c3_15280), PpRALF2 (Pp3c6_7200)
547 and PpRALF3 (Pp3c25_4180) in the immune response. Previously, PpRALF1 and PpRALF2
548 have been shown to promote protonema tip growth and elongation (Ginanjar et al., 2022).
549 According to our findings, the knockout of all three *PpRALF* genes led to consistent changes
550 in plant proteomes, suggesting that all three PpRALFs are functional. For example, a
551 predicted metalloproteinase Pp3c15_830 was significantly downregulated in all *PpRALF*
552 knockout lines. Plant metalloproteinases are shown to be involved in growth, development,
553 and immunity (Flinn, 2008; Mishra et al., 2021).

554 The role of RALF peptides in stress response is mainly explored in the context of
555 Arabidopsis biology. In Arabidopsis, several RALF peptides have shown the ability to
556 modulate elf18-induced ROS production (Abarca et al., 2021). Based the amino acid
557 compositions, we clustered PpRALFs with AtRALFs, such as AtRALF23 and AtRALF33,
558 that negatively regulate immune response and inhibit elf18-induced ROS production in
559 Arabidopsis (Stegmann et al., 2017; Abarca et al., 2021). In addition, the AtRALF23 and
560 AtRALF33 were shown to interfere PAMP-triggered immunity (PTI) by binding to receptor
561 FER-LLG1 complex and inhibition of its scaffold function (Shen et al., 2017; Rzemieniewski
562 and Stegmann, 2022). AtRALF23 overexpression increases susceptibility to *Pseudomonas*
563 *syringae* pv. *tomato* DC3000 and to the fungus *Plectosphaerella cucumerina* (Stegmann et
564 al., 2017) and LRX3/4/5-RALF22/23-FER module negatively regulates the levels of
565 jasmonic acid (JA), salicylic acid (SA) and abscisic acid (ABA) in Arabidopsis (Zhao et al.,
566 2021). The hallmark of AtRALFs, that negatively regulate immune response, is the dibasic
567 site "RR" for subtilase S1P (Srivastava et al., 2009; Stegmann et al., 2017; Abarca et al.,
568 2021). However, there are some exceptions from this rule in Arabidopsis. In *P. patens*, only
569 PpRALF1 protein precursor contains the corresponding "RRLL" motif (Ginanjar et al.,
570 2022). According to our data, the PpRALF1 peptide has no role in stress response, but the
571 knockouts of two *PpRALFs* (2 and 3) resulted in increasing resistance to bacterial and fungal
572 pathogens - *P. carotovorum* and *F. solani*, suggesting the negative regulation of immune
573 response by these peptides. These PpRALFs are also placed in a distinct group on the
574 phylogenetic tree (Ginanjar et al., 2022).

575 In land plants, the immune response resulted in extensive transcriptome reprogramming
576 (Bjornson et al., 2021; Campos et al., 2021; Reboledo et al., 2021). The early transcriptome
577 changes include upregulation of genes involved in response to chitin and wounding at 5 min
578 and participated in response to hydrogen peroxide and cell wall modification at 180 min after
579 treatment by known elicitors in the model plant Arabidopsis (Bjornson et al., 2021). In our
580 study, we found that transcriptome reprogramming in wild type *P. patens* plants at 7 dpi
581 affected genes that participate in response to reactive oxygen species (GO:0000302),
582 polyketide metabolic process (GO:0030638), phenylpropanoid metabolic process
583 (GO:0009698), cinnamic acid metabolic process (GO:0009803). It has been shown that ROS
584 level rises quickly in *P. patens* cells during *B. cinerea* infection and plays a role as second
585 messengers during the moss immunity (Ponce de León et al. 2012). In addition, the moss *P.*
586 *patens* responds to the fungal pathogen *B. cinerea* by reinforces the cell wall, upregulating
587 the genes involved in defense response and activation of the shikimate and phenylpropanoid
588 pathways (Ponce De León et al., 2012; Castro et al., 2016; Reboledo et al., 2021). The
589 *Marchantia* response to oomycete infection is also based on the phenylpropanoid-mediated

590 biochemical defenses that suggest this mechanism as a hallmark of an ancestral pathogen
591 deterrence strategy (Carella et al., 2019).

592 Even though the difference in the pathogenic agent - *B. cinerea* (necrotrophic fungus) vs *F.*
593 *solani* (facultative parasite) and time after inoculation when samples were collected - 24-h vs
594 7 dpi, about 40% of DEGs in wild type plants from our data were identical to the Reboledo
595 dataset (Reboledo et al., 2021). However, the overlap between DEGs from *PpRALF3* KO
596 plants and the aforementioned dataset was only 27%, suggesting specific immune responses
597 in the knockout line.

598 Because our ultimate goal was to understand the role of PpRALFs in stress response, we
599 concentrated on the comparison of the transcriptomes between wild type and *PpRALF3*
600 knockout plants during *F. solani* infection. About 40% of *PpRALF3* KO DEGs were identical
601 to wild type DEGs and changed in similar manner. The corresponding GO terms belonged to
602 oxidoreductase activity (GO:0016491), response to reactive oxygen species (GO:0000302),
603 antioxidant activity (GO:0016209). This finding is in line with previous studies on vascular
604 and non-vascular plants in which increased expression of oxidative stress related genes
605 encoding peroxiredoxins, thioredoxins, ferredoxins during infection was detected (Ponce de
606 León, 2011; Bjornson et al., 2021; Reboledo et al., 2021). According to our results, the
607 *PpRALF3* KO DEGs were not enriched in phenylpropanoid and cinnamic acid metabolic
608 processes as we observed in wild type plants, but some genes involved in the flavonoid
609 biosynthetic process, such as chalcone synthases, were upregulated in mutant lines.
610 Importantly, the *PpRALF2* KO and *PpRALF3* KO lines were less infected by *F. solani* than
611 wild type plants and *PpRALF1* KO genotype suggest their increased resistance. Therefore,
612 the transcriptome differences between wild type and *PpRALF3* KO plants might reflect
613 reduced propagation of *F. solani* in knockout lines. In contrast to wild type plants, a group of
614 genes involved in the pectin catabolic process, such as pectate lyases and pectin esterases,
615 were significantly downregulated in the *PpRALF3* KO plants under infection. Pectins are
616 structural heteropolysaccharides and major components of the plant primary cell wall
617 involved in maintaining plant growth and development, morphogenesis, defense responses,
618 etc. (Hongo et al., 2012; Leng et al., 2017). The pectin-degrading enzymes cause plant tissue
619 maceration, cell lysis and modification of the cell wall structure (Atanasova et al., 2018). Our
620 findings is corroborate with the previous findings that salt stress resulted in downregulation
621 of genes involved in cell wall organization and modification processes, such as pectin lyase-
622 like superfamily proteins, expansins, xyloglucan hydrolases in *lrx345* (lrx3, 4, 5 triple
623 mutants) Arabidopsis plants (Zhao et al., 2021). LRX8-LRX11 proteins are shown to interact
624 with RALF4/19 and regulate pollen germination and pollen tube growth in Arabidopsis
625 (Mecchia et al., 2017). The downregulation of similar cell wall related genes in our *PpRALF3*
626 knockout line under stress conditions suggest the role of RALF peptides and the cognate
627 receptors, such as FERONIA or LRXs, as modules that integrate plant growth and stress
628 tolerance regulation in land plants.

629 In addition, it has been shown that pectin methylesterification is a subject of regulation
630 during response to phytopathogens and a high level of pectin methylesterification correlated
631 with an increased resistance to pathogens (Wydra and Beri, 2006; Lionetti et al., 2012). In
632 Arabidopsis, downregulation of some pectin methylesterases during *B. cinerea* infection
633 probably represent a defense mechanism to limit pectin demethylesterification and its
634 subsequent degradation by fungal enzymes (Lionetti et al., 2017). Together with our results
635 on the increased cell wall regeneration in *PpRALF2* and *PpRALF3* KO protoplasts relative to
636 wild type cells, it may point to changes in cell wall composition as an important factor of

637 increased resistance to phytopathogens in the corresponding knockout lines. There is no
638 direct evidence how different RALF peptides influence cell wall composition in plants, but
639 knockout of some LRXs in Arabidopsis resulted in the increase of mannose and lignin if
640 compared with wild type plants (Draeger et al., 2015). Taken together, our findings suggest
641 the role of PpRALF2 and PpRALF3 peptides in negative regulation of *P. patens* immune
642 response.

643 We observed that *PpRALF3* and both double KO mutant lines were more tolerant to growth
644 inhibition under salt and oxidative stress conditions. Previously, the role of AtRALF22 or
645 AtRALF23 and their cognate receptors in coordinated regulation of cell wall integrity,
646 growth and salt stress response was demonstrated in Arabidopsis (Zhao et al., 2018, 2021).
647 The overexpression of AtRALF22 or AtRALF23 are shown to increase sensitivity to salt
648 stress (Zhao et al., 2018). Moreover, LRX3/4/5-RALF22/23-FER module is shown to
649 regulate hormonal homeostasis and ROS accumulation in Arabidopsis. Thus, our findings are
650 in line with previous studies on flowering plants and show that RALF peptides in the non-
651 vascular plants can also participate in abiotic stress response, modulating plant growth in
652 such conditions. The detailed mechanisms through which ancient RALF and their cognate
653 receptors coordinated plant growth, cell wall integrity and response to distinct environmental
654 changes (e.g., pathogen invasion) is unknown. However, the future study on genetically
655 redundant plants, such as *P. patens*, can help elucidate the evolution and exact mechanisms of
656 RALF peptides signaling.

657 **5 Data availability statement**

658 The nucleotide sequence reported in this paper has been submitted to NCBI Sequence Reads
659 Archive (SRA) with accession number PRJNA879762. The mass spectrometry proteomics
660 data have been deposited to the ProteomeXchange Consortium via the PRIDE (Perez-Riverol
661 et al., 2022) partner repository with the dataset identifier PXD037111.

662 **Username:** reviewer_pxd037111@ebi.ac.uk

663 **Password:** 7qCU3gkd

664 **6 Author contributions**

665 AM, IL, IF wrote the manuscript. AM, IL, NG conducted all experiments and contributed to
666 data analysis. IF performed data analysis and supervised the study. AK, VL and DKh
667 conducted generation of knockout moss lines, also AK contributed to growth and
668 morphological experiments. TM, ECh, SE performed pathogens inoculation and moss
669 treatment. VV, KK, TG and VB performed RNA-seq analysis.

670 **7 Funding**

671

672 **8 Conflict of interest**

673 The authors declare that the research was conducted in the absence of any commercial or
674 financial relationships that could be construed as a potential conflict of interest.

675 **9 Acknowledgments**

676 We thank the Center for Precision Genome Editing and Genetic Technologies for Biomedicine,
677 Federal Research and Clinical Center of Physical-Chemical Medicine of the Federal Medical
678 Biological Agency for the expertise and guidance in genetic engineering.

679 **10 Supplementary material**

680 **11 References**

681 Abarca, A., Franck, C. M., and Zipfel, C. (2021). Family-wide evaluation of RAPID
682 ALKALINIZATION FACTOR peptides. *Plant Physiol.* 187, 996–1010.

683 Akita, M., Lehtonen, M. T., Koponen, H., Marttinen, E. M., and Valkonen, J. P. T. (2011). Infection
684 of the Sunagoke moss panels with fungal pathogens hampers sustainable greening in urban
685 environments. *Sci. Total Environ.* 409, 3166–3173.

686 Alvarez, A., Montesano, M., Schmelz, E., and Ponce de León, I. (2016). Activation of Shikimate,
687 Phenylpropanoid, Oxylipins, and Auxin Pathways in Pectobacterium carotovorum Elicitors-
688 Treated Moss. *Front. Plant Sci.* 7, 328.

689 Atanasova, L., Dubey, M., Grujić, M., Gudmundsson, M., Lorenz, C., Sandgren, M., et al. (2018).
690 Evolution and functional characterization of pectate lyase PEL12, a member of a highly
691 expanded Clonostachys rosea polysaccharide lyase 1 family. *BMC Microbiol.* 18, 178.

692 Atkinson, N. J., Lilley, C. J., and Urwin, P. E. (2013). Identification of genes involved in the response
693 of Arabidopsis to simultaneous biotic and abiotic stresses. *Plant Physiol.* 162, 2028–2041.

694 Bjornson, M., Pimprikar, P., Nürnberger, T., and Zipfel, C. (2021). The transcriptional landscape of
695 Arabidopsis thaliana pattern-triggered immunity. *Nat Plants* 7, 579–586.

696 Blackburn, M. R., Haruta, M., and Moura, D. S. (2020). Twenty Years of Progress in Physiological
697 and Biochemical Investigation of RALF Peptides. *Plant Physiol.* 182, 1657–1666.

698 Bolger, A. M., Lohse, M., and Usadel, B. (2014). Trimmomatic: a flexible trimmer for Illumina
699 sequence data. *Bioinformatics* 30, 2114–2120.

700 Campbell, L., and Turner, S. R. (2017). A Comprehensive Analysis of RALF Proteins in Green Plants
701 Suggests There Are Two Distinct Functional Groups. *Front. Plant Sci.* 8, 37.

702 Campos, M. D., Félix, M. do R., Patanita, M., Materatski, P., and Varanda, C. (2021). High
703 throughput sequencing unravels tomato-pathogen interactions towards a sustainable plant
704 breeding. *Hortic Res* 8, 171.

705 Cao, J., and Shi, F. (2012). Evolution of the RALF Gene Family in Plants: Gene Duplication and
706 Selection Patterns. *Evol. Bioinform. Online* 8, 271–292.

707 Carella, P., Gogleva, A., Hoey, D. J., Bridgen, A. J., Stolze, S. C., Nakagami, H., et al. (2019).
708 Conserved Biochemical Defenses Underpin Host Responses to Oomycete Infection in an Early-
709 Divergent Land Plant Lineage. *Curr. Biol.* 29, 2282–2294.e5.

710 Castro, A., Vidal, S., and Ponce de León, I. (2016). Moss Pathogenesis-Related-10 Protein Enhances
711 Resistance to Pythium irregulare in Physcomitrella patens and Arabidopsis thaliana. *Front. Plant*
712 *Sci.* 7, 580.

713 Chen, Z., Zhao, P., Li, F., Leier, A., Marquez-Lago, T. T., Wang, Y., et al. (2018). iFeature: a Python

714 package and web server for features extraction and selection from protein and peptide sequences.
715 *Bioinformatics* 34, 2499–2502.

716 Chevalier, E., Loubert-Hudon, A., and Matton, D. P. (2013). ScRALF3, a secreted RALF-like peptide
717 involved in cell-cell communication between the sporophyte and the female gametophyte in a
718 solanaceous species. *Plant J.* 73, 1019–1033.

719 Collonnier, C., Epert, A., Mara, K., Maclot, F., Guyon-Debast, A., Charlot, F., et al. (2017). CRISPR-
720 Cas9-mediated efficient directed mutagenesis and RAD51-dependent and RAD51-independent
721 gene targeting in the mossPhyscomitrella patens. *Plant Biotechnol. J.* 15, 122–131.

722 Draeger, C., Ndinyanka Fabrice, T., Gineau, E., Mouille, G., Kuhn, B. M., Moller, I., et al. (2015).
723 Arabidopsis leucine-rich repeat extensin (LRX) proteins modify cell wall composition and
724 influence plant growth. *BMC Plant Biol.* 15, 155.

725 Faurobert, M., Pelpoir, E., and Chaïb, J. (2007). Phenol extraction of proteins for proteomic studies of
726 recalcitrant plant tissues. *Methods Mol. Biol.* 355, 9–14.

727 Fesenko, I. A., Arapidi, G. P., Skripnikov, A. Y., Alexeev, D. G., Kostryukova, E. S., Manolov, A. I.,
728 et al. (2015). Specific pools of endogenous peptides are present in gametophore, protonema, and
729 protoplast cells of the moss Physcomitrella patens. *BMC Plant Biol.* 15, 87.

730 Fesenko, I., Kirov, I., Kniazev, A., Khazigaleeva, R., Lazarev, V., Kharlampieva, D., et al. (2019).
731 Distinct types of short open reading frames are translated in plant cells. *Genome Res.* 29, 1464–
732 1477.

733 Fesenko, I., Shabalina, S. A., Mamaeva, A., Knyazev, A., Glushkevich, A., Lyapina, I., et al. (2021a).
734 A vast pool of lineage-specific microproteins encoded by long non-coding RNAs in plants.
735 *Nucleic Acids Res.* 49, 10328–10346.

736 Fesenko, I., Spechenkova, N., Mamaeva, A., Makhotenko, A. V., Love, A. J., Kalinina, N. O., et al.
737 (2021b). Role of the methionine cycle in the temperature-sensitive responses of potato plants to
738 potato virus Y. *Mol. Plant Pathol.* 22, 77–91.

739 Flinn, B. S. (2008). Plant extracellular matrix metalloproteinases. *Funct. Plant Biol.* 35, 1183–1193.

740 Franck, C. M., Westermann, J., and Boisson-Dernier, A. (2018). Plant Malectin-Like Receptor
741 Kinases: From Cell Wall Integrity to Immunity and Beyond. *Annu. Rev. Plant Biol.* 69, 301–328.

742 Frederick, R. O., Haruta, M., Tonelli, M., Lee, W., Cornilescu, G., Cornilescu, C. C., et al. (2019).
743 Function and solution structure of the Arabidopsis thaliana RALF8 peptide. *Protein Sci.* 28,
744 1115–1126.

745 Ge, Z., Bergonci, T., Zhao, Y., Zou, Y., Du, S., Liu, M.-C., et al. (2017). Arabidopsis pollen tube
746 integrity and sperm release are regulated by RALF-mediated signaling. *Science* 358, 1596–1600.

747 Ge, Z., Dresselhaus, T., and Qu, L.-J. (2019). How CrRLK1L Receptor Complexes Perceive RALF
748 Signals. *Trends Plant Sci.* 24, 978–981.

749 Ginanjar, E. F., Teh, O.-K., and Fujita, T. (2022). Characterisation of rapid alkalinisation factors in
750 Physcomitrium patens reveals functional conservation in tip growth. *New Phytol.* 233, 2442–
751 2457.

752 Herrera-Ubaldo, H., and de Folter, S. (2018). Exploring Cell Wall Composition and Modifications
753 During the Development of the Gynoecium Medial Domain in Arabidopsis. *Front. Plant Sci.* 9,
754 454.

755 Hoang, Q. T., Cho, S. H., McDaniel, S. F., Ok, S. H., Quatrano, R. S., and Shin, J. S. (2009). An
756 actinoporin plays a key role in water stress in the moss Physcomitrella patens. *New Phytol.* 184,
757 502–510.

758 Hongo, S., Sato, K., Yokoyama, R., and Nishitani, K. (2012). Demethylesterification of the primary
759 wall by PECTIN METHYLESTERASE35 provides mechanical support to the Arabidopsis stem.
760 *Plant Cell* 24, 2624–2634.

761 Kabir, M. N., Taheri, A., and Dumenyo, C. K. (2020). Development of PCR-Based Detection System
762 for Soft Rot Pectobacteriaceae Pathogens Using Molecular Signatures. *Microorganisms* 8. doi:
763 10.3390/microorganisms8030358.

764 Katoh, K., Rozewicki, J., and Yamada, K. D. (2019). MAFFT online service: multiple sequence
765 alignment, interactive sequence choice and visualization. *Brief. Bioinform.* 20, 1160–1166.

766 Khraiwesh, B., Qudeimat, E., Thimma, M., Chaiboonchoe, A., Jijakli, K., Alzahmi, A., et al. (2015).
767 Genome-wide expression analysis offers new insights into the origin and evolution of
768 Physcomitrella patens stress response. *Sci. Rep.* 5, 17434.

769 Kim, D., Langmead, B., and Salzberg, S. L. (2015). HISAT: a fast spliced aligner with low memory
770 requirements. *Nat. Methods* 12, 357–360.

771 Kolberg, L., Raudvere, U., Kuzmin, I., Vilo, J., and Peterson, H. (2020). gprofiler2 -- an R package
772 for gene list functional enrichment analysis and namespace conversion toolset g:Profiler.
773 *F1000Res.* 9. doi: 10.12688/f1000research.24956.2.

774 Lang, D., Ullrich, K. K., Murat, F., Fuchs, J., Jenkins, J., Haas, F. B., et al. (2018). The
775 Physcomitrella patens chromosome-scale assembly reveals moss genome structure and
776 evolution. *Plant J.* 93, 515–533.

777 Leng, Y., Yang, Y., Ren, D., Huang, L., Dai, L., Wang, Y., et al. (2017). A Rice PECTATE LYASE-
778 LIKE Gene Is Required for Plant Growth and Leaf Senescence. *Plant Physiol.* 174, 1151–1166.

779 Liao, Y., Smyth, G. K., and Shi, W. (2014). featureCounts: an efficient general purpose program for
780 assigning sequence reads to genomic features. *Bioinformatics* 30, 923–930.

781 Li, C., Yeh, F.-L., Cheung, A. Y., Duan, Q., Kita, D., Liu, M.-C., et al. (2015).
782 Glycosylphosphatidylinositol-anchored proteins as chaperones and co-receptors for FERONIA
783 receptor kinase signaling in Arabidopsis. *Elife* 4. doi: 10.7554/eLife.06587.

784 Li, H., Handsaker, B., Wysoker, A., Fennell, T., Ruan, J., Homer, N., et al. (2009). The Sequence
785 Alignment/Map format and SAMtools. *Bioinformatics* 25, 2078–2079.

786 Lionetti, V., Cervone, F., and Bellincampi, D. (2012). Methyl esterification of pectin plays a role
787 during plant–pathogen interactions and affects plant resistance to diseases. *J. Plant Physiol.* 169,
788 1623–1630.

789 Lionetti, V., Fabri, E., De Caroli, M., Hansen, A. R., Willats, W. G. T., Piro, G., et al. (2017). Three
790 Pectin Methylesterase Inhibitors Protect Cell Wall Integrity for Arabidopsis Immunity to
791 Botrytis. *Plant Physiol.* 173, 1844–1863.

792 Loubert-Hudon, A., Mazin, B. D., Chevalier, É., and Matton, D. P. (2020). The ScRALF3 secreted
793 peptide is involved in sporophyte to gametophyte signalling and affects pollen mitosis I. *Plant*
794 *Biol.* 22, 13–20.

795 Maksimov, N. M., Breigin, M. A., and Ermakov, I. P. (2016). Regulation of ion transport across the
796 pollen tube plasmalemma by hydrogen peroxide. *Cell tissue biol.* 10, 69–75.

797 McKinney, W. (2012). *Python for Data Analysis: Data Wrangling with Pandas, NumPy, and IPython*.
798 "O'Reilly Media, Inc."

799 Mecchia, M. A., Santos-Fernandez, G., Duss, N. N., Somoza, S. C., Boisson-Dernier, A., Gagliardini,
800 V., et al. (2017). RALF4/19 peptides interact with LRX proteins to control pollen tube growth in
801 Arabidopsis. *Science* 358, 1600–1603.

802 Merino, M. C., Guidarelli, M., Negrini, F., De Biase, D., Pession, A., and Baraldi, E. (2019). Induced
803 expression of the Fragaria × ananassa Rapid alkalinization factor-33-like gene decreases
804 anthracnose ontogenic resistance of unripe strawberry fruit stages. *Mol. Plant Pathol.* 20, 1252–
805 1263.

806 Mishra, L. S., Kim, S.-Y., Caddell, D. F., Coleman-Derr, D., and Funk, C. (2021). Loss of
807 Arabidopsis matrix metalloproteinase-5 affects root development and root bacterial communities
808 during drought stress. *Physiol. Plant.* 172, 1045–1058.

809 Moussu, S., Broyart, C., Santos-Fernandez, G., Augustin, S., Wehrle, S., Grossniklaus, U., et al.
810 (2020). Structural basis for recognition of RALF peptides by LRX proteins during pollen tube
811 growth. *Proc. Natl. Acad. Sci. U. S. A.* 117, 7494–7503.

812 Murphy, E., and De Smet, I. (2014). Understanding the RALF family: a tale of many species. *Trends*
813 *Plant Sci.* 19, 664–671.

814 Olsson, V., Joos, L., Zhu, S., Gevaert, K., Butenko, M. A., and De Smet, I. (2019). Look Closely, the
815 Beautiful May Be Small: Precursor-Derived Peptides in Plants. *Annu. Rev. Plant Biol.* 70, 153–
816 186.

817 Ow, S. Y., Salim, M., Noirel, J., Evans, C., Rehman, I., and Wright, P. C. (2009). iTRAQ
818 Underestimation in Simple and Complex Mixtures: "The Good, the Bad and the Ugly." *J.*
819 *Proteome Res.* 8, 5347–5355.

820 Perez-Riverol, Y., Bai, J., Bandla, C., García-Seisdedos, D., Hewapathirana, S., Kamatchinathan, S.,
821 et al. (2022). The PRIDE database resources in 2022: a hub for mass spectrometry-based
822 proteomics evidences. *Nucleic Acids Res.* 50, D543–D552.

823 Ponce de León, I. (2011). The Moss Physcomitrella patens as a Model System to Study Interactions
824 between Plants and Phytopathogenic Fungi and Oomycetes. *J. Pathog.* 2011, 719873.

825 Ponce De León, I., Schmelz, E. A., Gaggero, C., Castro, A., Álvarez, A., and Montesano, M. (2012).
826 Physcomitrella patens activates reinforcement of the cell wall, programmed cell death and
827 accumulation of evolutionary conserved defence signals, such as salicylic acid and 12-oxo-
828 phytodienoic acid, but not jasmonic acid, upon Botrytis cinerea infection. *Mol. Plant Pathol.* 13,
829 960–974.

830 Raudvere, U., Kolberg, L., Kuzmin, I., Arak, T., Adler, P., Peterson, H., et al. (2019). g:Profiler: a
831 web server for functional enrichment analysis and conversions of gene lists (2019 update).
832 *Nucleic Acids Res.* 47, W191–W198.

833 Reboledo, G., Agorio, A. D., Vignale, L., Batista-García, R. A., and Ponce De León, I. (2021).
834 Transcriptional profiling reveals conserved and species-specific plant defense responses during
835 the interaction of Physcomitrium patens with Botrytis cinerea. *Plant Mol. Biol.* 107, 365–385.

836 Robinson, M. D., McCarthy, D. J., and Smyth, G. K. (2010). edgeR: a Bioconductor package for
837 differential expression analysis of digital gene expression data. *Bioinformatics* 26, 139–140.

838 Rzemieniewski, J., and Stegmann, M. (2022). Regulation of pattern-triggered immunity and growth

839 by phytocytokines. *Curr. Opin. Plant Biol.* 68, 102230.

840 Schaefer, D. G., and Zrÿd, J. P. (1997). Efficient gene targeting in the moss Physcomitrella patens.
841 *Plant J.* 11, 1195–1206.

842 Schessner, J. P., Voytik, E., and Bludau, I. (2022). A practical guide to interpreting and generating
843 bottom-up proteomics data visualizations. *Proteomics* 22, e2100103.

844 Shannon, P., Markiel, A., Ozier, O., Baliga, N. S., Wang, J. T., Ramage, D., et al. (2003). Cytoscape:
845 a software environment for integrated models of biomolecular interaction networks. *Genome*
846 *Res.* 13, 2498–2504.

847 Shen, Q., Bourdais, G., Pan, H., Robatzek, S., and Tang, D. (2017). Arabidopsis
848 glycosylphosphatidylinositol-anchored protein LLG1 associates with and modulates FLS2 to
849 regulate innate immunity. *Proc. Natl. Acad. Sci. U. S. A.* 114, 5749–5754.

850 Solis-Miranda, J., Fonseca-García, C., Nava, N., Pacheco, R., and Quinto, C. (2020). Genome-Wide
851 Identification of the CrRLK1L Subfamily and Comparative Analysis of Its Role in the Legume-
852 Rhizobia Symbiosis. *Genes* 11. doi: 10.3390/genes11070793.

853 Srivastava, R., Liu, J.-X., Guo, H., Yin, Y., and Howell, S. H. (2009). Regulation and processing of a
854 plant peptide hormone, AtRALF23, in Arabidopsis. *Plant J.* 59, 930–939.

855 Stegmann, M., Monaghan, J., Smakowska-Luzan, E., Rovenich, H., Lehner, A., Holton, N., et al.
856 (2017). The receptor kinase FER is a RALF-regulated scaffold controlling plant immune
857 signaling. *Science* 355, 287–289.

858 Szklarczyk, D., Franceschini, A., Wyder, S., Forslund, K., Heller, D., Huerta-Cepas, J., et al. (2014).
859 STRING v10: protein–protein interaction networks, integrated over the tree of life. *Nucleic Acids*
860 *Res.* 43, D447–D452.

861 Tena, G. (2016). Immunity: RALF to the rescue. *Nat Plants* 2, 16067.

862 Thynne, E., Saur, I. M. L., Simbaqueba, J., Ogilvie, H. A., Gonzalez-Cendales, Y., Mead, O., et al.
863 (2017). Fungal phytopathogens encode functional homologues of plant rapid alkalinization factor
864 (RALF) peptides. *Mol. Plant Pathol.* 18, 811–824.

865 Van Rossum, G., and Drake, F. L., Jr (1995). Python tutorial: Centrum voor Wiskunde en Informatica
866 Amsterdam. *The Netherlands*.

867 Vidali, L., and Bezanilla, M. (2012). Physcomitrella patens: a model for tip cell growth and
868 differentiation. *Curr. Opin. Plant Biol.* 15, 625–631.

869 Virtanen, P., Gommers, R., Oliphant, T. E., Haberland, M., Reddy, T., Cournapeau, D., et al. (2020).
870 SciPy 1.0: fundamental algorithms for scientific computing in Python. *Nat. Methods* 17, 261–
871 272.

872 Waskom, M. (2021). seaborn: statistical data visualization. *J. Open Source Softw.* 6, 3021.

873 Waterhouse, A. M., Procter, J. B., Martin, D. M. A., Clamp, M., and Barton, G. J. (2009). Jalview
874 Version 2--a multiple sequence alignment editor and analysis workbench. *Bioinformatics* 25,
875 1189–1191.

876 Wieghaus, A., Prüfer, D., and Schulze Gronover, C. (2019). Loss of function mutation of the Rapid
877 Alkalinization Factor (RALF1)-like peptide in the dandelion Taraxacum koksaghyz entails a
878 high-biomass taproot phenotype. *PLoS One* 14, e0217454.

879 Wood, A. K. M., Walker, C., Lee, W.-S., Urban, M., and Hammond-Kosack, K. E. (2020). Functional
880 evaluation of a homologue of plant rapid alkalinisation factor (RALF) peptides in Fusarium
881 graminearum. *Fungal Biol.* 124, 753–765.

882 Wydra, K., and Beri, H. (2006). Structural changes of homogalacturonan, rhamnogalacturonan I and
883 arabinogalactan protein in xylem cell walls of tomato genotypes in reaction to Ralstonia
884 solanacearum. *Physiol. Mol. Plant Pathol.* 68, 41–50.

885 Xiao, Y., Stegmann, M., Han, Z., DeFalco, T. A., Parys, K., Xu, L., et al. (2019). Mechanisms of
886 RALF peptide perception by a heterotypic receptor complex. *Nature* 572, 270–274.

887 Zhang, X., Peng, H., Zhu, S., Xing, J., Li, X., Zhu, Z., et al. (2020a). Nematode-Encoded RALF
888 Peptide Mimics Facilitate Parasitism of Plants through the FERONIA Receptor Kinase. *Mol.*
889 *Plant* 13, 1434–1454.

890 Zhang, X., Yang, Z., Wu, D., and Yu, F. (2020b). RALF–FERONIA Signaling: Linking Plant
891 Immune Response with Cell Growth. *Plant Communications* 1, 100084.

892 Zhao, C., Jiang, W., Zayed, O., Liu, X., Tang, K., Nie, W., et al. (2021). The LRXs-RALFs-FER
893 module controls plant growth and salt stress responses by modulating multiple plant hormones.
894 *Natl Sci Rev* 8, nwaa149.

895 Zhao, C., Zayed, O., Yu, Z., Jiang, W., Zhu, P., Hsu, C.-C., et al. (2018). Leucine-rich repeat extensin
896 proteins regulate plant salt tolerance in Arabidopsis. *Proc. Natl. Acad. Sci. U. S. A.* 115, 13123–
897 13128.

898 Abarca, A., Franck, C. M., and Zipfel, C. (2021). Family-wide evaluation of RAPID
899 ALKALINIZATION FACTOR peptides. Plant Physiol. 187, 996–1010.

900 Akita, M., Lehtonen, M. T., Koponen, H., Marttinen, E. M., and Valkonen, J. P. T. (2011). Infection
901 of the Sunagoke moss panels with fungal pathogens hampers sustainable greening in urban
902 environments. Sci. Total Environ. 409, 3166–3173.

903 Alvarez, A., Montesano, M., Schmelz, E., and Ponce de León, I. (2016). Activation of Shikimate,
904 Phenylpropanoid, Oxylipins, and Auxin Pathways in Pectobacterium carotovorum Elicitors-
905 Treated Moss. Front. Plant Sci. 7, 328.

906 Atanasova, L., Dubey, M., Grujić, M., Gudmundsson, M., Lorenz, C., Sandgren, M., et al. (2018).
907 Evolution and functional characterization of pectate lyase PEL12, a member of a highly
908 expanded Clonostachys rosea polysaccharide lyase 1 family. BMC Microbiol. 18, 178.

909 Atkinson, N. J., Lilley, C. J., and Urwin, P. E. (2013). Identification of genes involved in the response
910 of Arabidopsis to simultaneous biotic and abiotic stresses. Plant Physiol. 162, 2028–2041.

911 Bjornson, M., Pimprikar, P., Nürnberger, T., and Zipfel, C. (2021). The transcriptional landscape of
912 Arabidopsis thaliana pattern-triggered immunity. Nat Plants 7, 579–586.

913 Blackburn, M. R., Haruta, M., and Moura, D. S. (2020). Twenty Years of Progress in Physiological
914 and Biochemical Investigation of RALF Peptides. Plant Physiol. 182, 1657–1666.

915 Bolger, A. M., Lohse, M., and Usadel, B. (2014). Trimmomatic: a flexible trimmer for Illumina
916 sequence data. Bioinformatics 30, 2114–2120.

917 Campbell, L., and Turner, S. R. (2017). A Comprehensive Analysis of RALF Proteins in Green Plants
918 Suggests There Are Two Distinct Functional Groups. Front. Plant Sci. 8, 37.

919 Campos, M. D., Félix, M. do R., Patanita, M., Materatski, P., and Varanda, C. (2021). High

920 throughput sequencing unravels tomato-pathogen interactions towards a sustainable plant
921 breeding. Hortic Res 8, 171.

922 Cao, J., and Shi, F. (2012). Evolution of the RALF Gene Family in Plants: Gene Duplication and
923 Selection Patterns. Evol. Bioinform. Online 8, 271–292.

924 Carella, P., Gogleva, A., Hoey, D. J., Bridgen, A. J., Stolze, S. C., Nakagami, H., et al. (2019).
925 Conserved Biochemical Defenses Underpin Host Responses to Oomycete Infection in an Early-
926 Divergent Land Plant Lineage. Curr. Biol. 29, 2282–2294.e5.

927 Castro, A., Vidal, S., and Ponce de León, I. (2016). Moss Pathogenesis-Related-10 Protein Enhances
928 Resistance to Pythium irregulare in Physcomitrella patens and Arabidopsis thaliana. Front. Plant
929 Sci. 7, 580.

930 Chen, Z., Zhao, P., Li, F., Leier, A., Marquez-Lago, T. T., Wang, Y., et al. (2018). iFeature: a Python
931 package and web server for features extraction and selection from protein and peptide sequences.
932 Bioinformatics 34, 2499–2502.

933 Chevalier, E., Loubert-Hudon, A., and Matton, D. P. (2013). ScRALF3, a secreted RALF-like peptide
934 involved in cell-cell communication between the sporophyte and the female gametophyte in a
935 solanaceous species. Plant J. 73, 1019–1033.

936 Draeger, C., Ndinyanka Fabrice, T., Gineau, E., Mouille, G., Kuhn, B. M., Moller, I., et al. (2015).
937 Arabidopsis leucine-rich repeat extensin (LRX) proteins modify cell wall composition and
938 influence plant growth. BMC Plant Biol. 15, 155.

939 Flinn, B. S. (2008). Plant extracellular matrix metalloproteinases. Funct. Plant Biol. 35, 1183–1193.

940 Franck, C. M., Westermann, J., and Boisson-Dernier, A. (2018). Plant Malectin-Like Receptor
941 Kinases: From Cell Wall Integrity to Immunity and Beyond. Annu. Rev. Plant Biol. 69, 301–
942 328.

943 Frederick, R. O., Haruta, M., Tonelli, M., Lee, W., Cornilescu, G., Cornilescu, C. C., et al. (2019).
944 Function and solution structure of the Arabidopsis thaliana RALF8 peptide. Protein Sci. 28,
945 1115–1126.

946 Ge, Z., Bergonci, T., Zhao, Y., Zou, Y., Du, S., Liu, M.-C., et al. (2017). Arabidopsis pollen tube
947 integrity and sperm release are regulated by RALF-mediated signaling. Science 358, 1596–1600.

948 Ge, Z., Dresselhaus, T., and Qu, L.-J. (2019). How CrRLK1L Receptor Complexes Perceive RALF
949 Signals. Trends Plant Sci. 24, 978–981.

950 Ginanjar, E. F., Teh, O.-K., and Fujita, T. (2022). Characterisation of rapid alkalinisation factors in
951 Physcomitrium patens reveals functional conservation in tip growth. New Phytol. 233, 2442–
952 2457.

953 Herrera-Ubaldo, H., and de Folter, S. (2018). Exploring Cell Wall Composition and Modifications
954 During the Development of the Gynoecium Medial Domain in Arabidopsis. Front. Plant Sci. 9,
955 454.

956 Hoang, Q. T., Cho, S. H., McDaniel, S. F., Ok, S. H., Quatrano, R. S., and Shin, J. S. (2009). An
957 actinoporin plays a key role in water stress in the moss Physcomitrella patens. New Phytol. 184,
958 502–510.

959 Hongo, S., Sato, K., Yokoyama, R., and Nishitani, K. (2012). Demethylesterification of the primary
960 wall by PECTIN METHYLESTERASE35 provides mechanical support to the Arabidopsis stem.
961 Plant Cell 24, 2624–2634.

962 Khraiwesh, B., Qudeimat, E., Thimma, M., Chaiboonchoe, A., Jijakli, K., Alzahmi, A., et al. (2015).
963 Genome-wide expression analysis offers new insights into the origin and evolution of
964 Physcomitrella patens stress response. Sci. Rep. 5, 17434.

965 Kim, D., Langmead, B., and Salzberg, S. L. (2015). HISAT: a fast spliced aligner with low memory
966 requirements. Nat. Methods 12, 357–360.

967 Kolberg, L., Raudvere, U., Kuzmin, I., Vilo, J., and Peterson, H. (2020). gprofiler2 -- an R package
968 for gene list functional enrichment analysis and namespace conversion toolset g:Profiler.
969 F1000Res. 9. doi: 10.12688/f1000research.24956.2.

970 Leng, Y., Yang, Y., Ren, D., Huang, L., Dai, L., Wang, Y., et al. (2017). A Rice PECTATE LYASE-
971 LIKE Gene Is Required for Plant Growth and Leaf Senescence. Plant Physiol. 174, 1151–1166.

972 Liao, Y., Smyth, G. K., and Shi, W. (2014). featureCounts: an efficient general purpose program for
973 assigning sequence reads to genomic features. Bioinformatics 30, 923–930.

974 Li, C., Yeh, F.-L., Cheung, A. Y., Duan, Q., Kita, D., Liu, M.-C., et al. (2015).
975 Glycosylphosphatidylinositol-anchored proteins as chaperones and co-receptors for FERONIA
976 receptor kinase signaling in Arabidopsis. Elife 4. doi: 10.7554/eLife.06587.

977 Li, H., Handsaker, B., Wysoker, A., Fennell, T., Ruan, J., Homer, N., et al. (2009). The Sequence
978 Alignment/Map format and SAMtools. Bioinformatics 25, 2078–2079.

979 Lionetti, V., Cervone, F., and Bellincampi, D. (2012). Methyl esterification of pectin plays a role
980 during plant–pathogen interactions and affects plant resistance to diseases. J. Plant Physiol. 169,
981 1623–1630.

982 Lionetti, V., Fabri, E., De Caroli, M., Hansen, A. R., Willats, W. G. T., Piro, G., et al. (2017). Three
983 Pectin Methylesterase Inhibitors Protect Cell Wall Integrity for Arabidopsis Immunity to
984 Botrytis. Plant Physiol. 173, 1844–1863.

985 Loubert-Hudon, A., Mazin, B. D., Chevalier, É., and Matton, D. P. (2020). The ScRALF3 secreted
986 peptide is involved in sporophyte to gametophyte signalling and affects pollen mitosis I. Plant
987 Biol. 22, 13–20.

988 Maksimov, N. M., Breigin, M. A., and Ermakov, I. P. (2016). Regulation of ion transport across the
989 pollen tube plasmalemma by hydrogen peroxide. Cell tissue biol. 10, 69–75.

990 Mecchia, M. A., Santos-Fernandez, G., Duss, N. N., Somoza, S. C., Boisson-Dernier, A., Gagliardini,
991 V., et al. (2017). RALF4/19 peptides interact with LRX proteins to control pollen tube growth in
992 Arabidopsis. Science 358, 1600–1603.

993 Merino, M. C., Guidarelli, M., Negrini, F., De Biase, D., Pession, A., and Baraldi, E. (2019). Induced
994 expression of the Fragaria × ananassa Rapid alkalinization factor-33-like gene decreases
995 anthracnose ontogenic resistance of unripe strawberry fruit stages. Mol. Plant Pathol. 20, 1252–
996 1263.

997 Mishra, L. S., Kim, S.-Y., Caddell, D. F., Coleman-Derr, D., and Funk, C. (2021). Loss of
998 Arabidopsis matrix metalloproteinase-5 affects root development and root bacterial communities
999 during drought stress. Physiol. Plant. 172, 1045–1058.

1000 Moussu, S., Broyart, C., Santos-Fernandez, G., Augustin, S., Wehrle, S., Grossniklaus, U., et al.
1001 (2020). Structural basis for recognition of RALF peptides by LRX proteins during pollen tube
1002 growth. Proc. Natl. Acad. Sci. U. S. A. 117, 7494–7503.

1003 Murphy, E., and De Smet, I. (2014). Understanding the RALF family: a tale of many species. Trends

1004 Plant Sci. 19, 664–671.

1005 Olsson, V., Joos, L., Zhu, S., Gevaert, K., Butenko, M. A., and De Smet, I. (2019). Look Closely, the
1006 Beautiful May Be Small: Precursor-Derived Peptides in Plants. Annu. Rev. Plant Biol. 70, 153–
1007 186.

1008 Perez-Riverol, Y., Bai, J., Bandla, C., García-Seisdedos, D., Hewapathirana, S., Kamatchinathan, S.,
1009 et al. (2022). The PRIDE database resources in 2022: a hub for mass spectrometry-based
1010 proteomics evidences. Nucleic Acids Res. 50, D543–D552.

1011 Ponce de León, I. (2011). The Moss Physcomitrella patens as a Model System to Study Interactions
1012 between Plants and Phytopathogenic Fungi and Oomycetes. J. Pathog. 2011, 719873.

1013 Ponce De León, I., Schmelz, E. A., Gaggero, C., Castro, A., Álvarez, A., and Montesano, M. (2012).
1014 Physcomitrella patens activates reinforcement of the cell wall, programmed cell death and
1015 accumulation of evolutionary conserved defence signals, such as salicylic acid and 12-oxo-
1016 phytodienoic acid, but not jasmonic acid, upon Botrytis cinerea infection. Mol. Plant Pathol. 13,
1017 960–974.

1018 Reboledo, G., Agorio, A. D., Vignale, L., Batista-García, R. A., and Ponce De León, I. (2021).
1019 Transcriptional profiling reveals conserved and species-specific plant defense responses during
1020 the interaction of Physcomitrium patens with Botrytis cinerea. Plant Mol. Biol. 107, 365–385.

1021 Robinson, M. D., McCarthy, D. J., and Smyth, G. K. (2010). edgeR: a Bioconductor package for
1022 differential expression analysis of digital gene expression data. Bioinformatics 26, 139–140.

1023 Rzemieniewski, J., and Stegmann, M. (2022). Regulation of pattern-triggered immunity and growth
1024 by phytocytokines. Curr. Opin. Plant Biol. 68, 102230.

1025 Shen, Q., Bourdais, G., Pan, H., Robatzek, S., and Tang, D. (2017). Arabidopsis
1026 glycosylphosphatidylinositol-anchored protein LLG1 associates with and modulates FLS2 to
1027 regulate innate immunity. Proc. Natl. Acad. Sci. U. S. A. 114, 5749–5754.

1028 Solis-Miranda, J., Fonseca-García, C., Nava, N., Pacheco, R., and Quinto, C. (2020). Genome-Wide
1029 Identification of the CrRLK1L Subfamily and Comparative Analysis of Its Role in the Legume-
1030 Rhizobia Symbiosis. Genes 11. doi: 10.3390/genes11070793.

1031 Srivastava, R., Liu, J.-X., Guo, H., Yin, Y., and Howell, S. H. (2009). Regulation and processing of a
1032 plant peptide hormone, AtRALF23, in Arabidopsis. Plant J. 59, 930–939.

1033 Stegmann, M., Monaghan, J., Smakowska-Luzan, E., Rovenich, H., Lehner, A., Holton, N., et al.
1034 (2017). The receptor kinase FER is a RALF-regulated scaffold controlling plant immune
1035 signaling. Science 355, 287–289.

1036 Tena, G. (2016). Immunity: RALF to the rescue. Nat Plants 2, 16067.

1037 Thynne, E., Saur, I. M. L., Simbaqueba, J., Ogilvie, H. A., Gonzalez-Cendales, Y., Mead, O., et al.
1038 (2017). Fungal phytopathogens encode functional homologues of plant rapid alkalinization factor
1039 (RALF) peptides. Mol. Plant Pathol. 18, 811–824.

1040 Vidali, L., and Bezanilla, M. (2012). Physcomitrella patens: a model for tip cell growth and
1041 differentiation. Curr. Opin. Plant Biol. 15, 625–631.

1042 Wieghaus, A., Prüfer, D., and Schulze Gronover, C. (2019). Loss of function mutation of the Rapid
1043 Alkalinization Factor (RALF1)-like peptide in the dandelion Taraxacum koksaghyz entails a
1044 high-biomass taproot phenotype. PLoS One 14, e0217454.

1045 Wood, A. K. M., Walker, C., Lee, W.-S., Urban, M., and Hammond-Kosack, K. E. (2020). Functional
1046 evaluation of a homologue of plant rapid alkalinisation factor (RALF) peptides in Fusarium
1047 graminearum. Fungal Biol. 124, 753–765.

1048 Wydra, K., and Beri, H. (2006). Structural changes of homogalacturonan, rhamnogalacturonan I and
1049 arabinogalactan protein in xylem cell walls of tomato genotypes in reaction to Ralstonia
1050 solanacearum. Physiol. Mol. Plant Pathol. 68, 41–50.

1051 Xiao, Y., Stegmann, M., Han, Z., DeFalco, T. A., Parys, K., Xu, L., et al. (2019). Mechanisms of
1052 RALF peptide perception by a heterotypic receptor complex. Nature 572, 270–274.

1053 Zhang, X., Peng, H., Zhu, S., Xing, J., Li, X., Zhu, Z., et al. (2020a). Nematode-Encoded RALF
1054 Peptide Mimics Facilitate Parasitism of Plants through the FERONIA Receptor Kinase. Mol.
1055 Plant 13, 1434–1454.

1056 Zhang, X., Yang, Z., Wu, D., and Yu, F. (2020b). RALF–FERONIA Signaling: Linking Plant
1057 Immune Response with Cell Growth. Plant Communications 1, 100084.

1058 Zhao, C., Jiang, W., Zayed, O., Liu, X., Tang, K., Nie, W., et al. (2021). The LRXs-RALFs-FER
1059 module controls plant growth and salt stress responses by modulating multiple plant hormones.
1060 Natl Sci Rev 8, nwaa149.

1061 Zhao, C., Zayed, O., Yu, Z., Jiang, W., Zhu, P., Hsu, C.-C., et al. (2018). Leucine-rich repeat extensin
1062 proteins regulate plant salt tolerance in Arabidopsis. Proc. Natl. Acad. Sci. U. S. A. 115, 13123–
1063 13128.

1064